ATF3 as a Key Regulator of Cisplatin Cytotoxicity: Combining ATF3 Inducing Agents Enhances Cisplatin Activity in NSCLC

Tabassom Baghai

Thesis submitted to the
Faculty of Graduate and Postdoctoral Studies
In partial fulfillment of the requirements
for the degree of Master's of Science in Biochemistry

Department of Biochemistry, Microbiology, and Immunology
Faculty of Medicine
University of Ottawa

Abstract

Lung cancer is the leading cause of cancer and cancer deaths worldwide, with non-small-cell lung carcinomas (NSCLC) representing 85% of all diagnosed lung cancers. Platinum-combination chemotherapy is the current standard treatment for NSCLC, however, associated toxicities and resistance limit its efficacy. Our laboratory previously identified activating transcription factor 3 (ATF3), a stress-inducible gene whose elevated and sustained expression can trigger apoptosis to a wide variety of stressors, as a key regulator of cisplatin cytotoxicity as well. Thus, enhanced and sustained induction of ATF3 by combining platins with other ATF3 inducers potentially represents an effective therapeutic strategy. A chemical library screen identified vorinostat and topotecan as ATF3 inducers that also enhance cisplatin cytotoxicity. ATF3 plays a significant role in cisplatin, vorinostat and topotecan and their combinations cytotoxicity. Importantly, vorinostat and topotecan induced synergistic cytotoxicity with cisplatin in NSCLC cell lines and their cisplatin resistance sub-lines with enhanced ATF3 expression observed. Our study suggests a potential novel therapeutic approach where ATF3 inducing agents in combination with platins represents a rational combination based therapeutic strategy.

Acknowledgements

I would like to thank Dr. Jim Dimitroulakos for his support and guidance throughout this project. Being a part of Dr. Dimitroulakos' laboratory gave me the opportunity to contribute to various different projects in the field of cancer therapeutics, which not only expanded my knowledge and skills, but also made me more appreciative of the impacts that the projects and experiments can have in a clinical setting.

I would also like to thank Dr. Christina Addison and Dr. Chantal Matar for the valuable feedback and guidance that they provided as members of my thesis advisory committee.

Thanks to Shaad Hasim, Lenah Mukhtar, Dr. Laurie Ma, and all the other wonderful colleagues that I had the pleasure of meeting during my time at the Ottawa Hospital Research Institute. I will forever be grateful for all the talks and advice that I received, both scientific and personal, and wish the best for all!

Lastly, I would like to thank my family and friends for the unconditional love and support. A special thank you to my mother, Jaleh, and my brothers, Arash and Sohrab, for always encouraging me to remain positive and to never give up! I would not have been able to complete this without you!

Table of Contents

List of Figures

List of Tables

LIST OF ABBREVIATIONS

ABC	ATP-binding cassette
AKI	Acute kidney injury
ALK	Anaplastic lymphoma kinase
AP-1	Activating protein 1
ATF	Activating transcription factor
ATM	Ataxia telangiectasia mutated
ATP7A	Copper-transporting P-type adenosine triphosphate 1
ATP7B	Copper-transporting P-type adenosine triphosphate 2
ATR	ATM and Rad-3 related
BAX	Bcl-2-associated X
Bcl-2	B-cell lymphoma 2
Bcl-XL	B-cell lymphoma-extra large
bZip	basic region-leucine zipper
c-Abl	v-abl Abelson murine leukaemia viral oncogene homologue
CDKI	Cyclin dependent kinase inhibitor
Chk	Checkpoint kinase
CHOP	C/EBP homologous protein
CI	Combination Index
Cisplatin	Cis-dichlorodiammineplatinum (II)
cisR	Cisplatin resistant
cPARP	Cleaved Poly(ADP-ribose) Polymerase
CREB	Cyclic AMP response element binding
CTR1	Copper transporter I
DDR	DNA damage response
DMEM	Dulbecco's Modified Eagle's Medium
Drg-1	Developmentally regulated GTP binding protein 1
DSB	Double-stranded breaks
EGFR	Epidermal growth factor receptor
elF2 α	Eukaryotic translation initiation factor 2 alpha
ER	Endoplasmic reticulum
ERCC1	Excision repair cross-complementing-1
ERK	Extracellular signal-regulated kinase
GADD153	Growth arrest DNA damage inducible 153
GADD153	Growth arrest DNA damage inducible gene 153
GS-X	Glutathione S-conjugate export
GSH	Glutathione
GST	Glutathione S-transferase
HDAC	Histone deacetylase
HDACi	Histone deacetylase inhibitor
IAP	Inhibitor of apoptosis
IR	Ionizing radiation
ISR	Integrated stress response
JNK	c-Jun N-terminal kinase

MAPK	Mitogen-activated protein kinase
MEF	Mouse embryonic fibroblast
MMP	Mitochondrial membrane potential
MMR	Mismatch repair
MRP	Multidrug resistance protein
MRP	Multidrug resistance protein
MTT	3-(4,5-Dimethylthiazol-2-yl)-2,5-Diphenyltetrazolium Bromide
NER	Nucleotide excision repair
NSCLC	Non-small cell lung cancer
OS	Overall survival
PARP	Poly(ADP-ribose) Polymerase
PBS	Phosphate buffered saline
Pol β	DNA polymerase β
PUMA	p53 upregulated modulator of apoptosis
ROS	Reactive oxygen species
SAHA	Suberoylanilide hydroxamic acid
SAPK	Stress-activated protein kinase
SCLC	Small cell lung cancer
SD	Standard deviation
TKI	Tyrosine kinase inhibitor
TLS	Translesion synthesis
UTR	Untranslated region
UV	Ultraviolet light
XIAP	X-linked inhibitor of apoptosis protein
XPF	Xeroderma pigmentosum complementation group

Chapter 1: Introduction

1.1 Non-small-cell lung cancer (NSCLC)

1.1.1 Background

Lung cancer is the most common cause of cancer malignancies worldwide, accounting for 12.9% of all new cancer diagnoses in 2012 [1]. It is recognized as a major health issue in Canada, with 28,600 new cases and 21,100 deaths estimated for the Canadian population in 2017 [2]. Additionally, lung cancer is responsible for a greater number of mortalities than the other three leading cancers, specifically breast, colorectal and pancreatic combined in Canada [2]. The five-year survival rate of this disease is approximately 17%, which is lower than a number of other commonly diagnosed cancers [2]. Lung cancer was once considered to be rare [3]; however, throughout the past century, it has grown into a global health issue that has instigated more studies to gain a thorough understanding of this disease [4,5].

Lung cancer can be divided into two subtypes, small cell lung cancer (SCLC) and non-small cell lung cancer (NSCLC), with NSCLC accounting for 85% of cases diagnosed [5]. NSCLC can be further classified into three histologic subtypes, adenocarcinoma, squamous cell carcinoma and large-cell carcinoma [5]. Adenocarcinoma is the most common type of NSCLC, accounting for 40% of cases [6]. It is diagnosed in both males and females, as well as in smokers and non-smokers [7,8] and typically emerges in the periphery of the lung [9], specifically from cells with glandular or secretory properties [8]. Although it is common, adenocarcinoma tends to grow at a slower rate relative to other subtypes, therefore, it is generally diagnosed at an

early stage [6]. Squamous cell carcinoma accounts for approximately 25-30% of lung cancer cases [6], and is strongly associated with the use of tobacco [10]. It generally arises from glandular or secretory cells in the airway epithelium, located in the center of the lungs, that undergo a metaplastic transformation that could be caused by various factors, including inflammation and exposure to tobacco [6,8]. Large cell carcinoma accounts for 5-10% of lung cancers and includes cases involving undifferentiated cells that lack the features associated with the other lung cancer subtypes [6,11]. This subtype is strongly linked to cigarette smoke exposure [12].

1.1.2 Risk factors

Tobacco smoking is widely recognized as a major risk factor for lung cancer [13]. The correlation between smoking and the rise in lung cancer diagnoses has been associated with the mass production and marketing of tobacco products beginning in the 20th century [14]. The length of time and the number of cigarettes an individual has smoked are known to impact the risk of cancer development [15]. A vast majority of lung cancer mortalities are due to smoking [13]; however, the rate of lung cancer incidences is expected to decrease in North America as there has been a gradual decrease in the number of smokers [13,16]. This suggests that lung cancer will become more prevalent among former or never smokers [16]. Moreover, passive smoking, also known as second-hand smoke, is also a risk factor, with spousal and workplace exposure to tobacco smoke linked to the development of lung cancer [17,18]. Another risk factor for lung cancer is exposure to air pollution, including emissions containing polycyclic aromatic hydrocarbons, which has been predicted to increase the risk of lung cancer mortality by

8% [19, 20]. Exposures to asbestos [21] and radon gas [22] have also been identified as risks for lung cancer.

Furthermore, a family history of lung cancer is a risk factor for both smokers and non-smokers [23]. Mutations occurring in the KRAS oncogene are responsible for 25-40% of lung adenocarcinoma cases [23]. Another key protein involved in many NSCLC cases is the epidermal growth factor receptor (EGFR), which plays a role in cell growth and division [24]. Overexpression or mutation status of EGFR can serve as predictive biomarkers of response to targeted therapies, such as tyrosine kinase inhibitors (TKIs) [25,26]. Mutations in the tumor protein p53, a tumor suppressor gene that also plays a role in regulating the cell cycle and apoptosis, have also been linked to lung cancer [27,28]. A study by Hwang et al. observed that carriers of the p53 mutations that also smoke are at a higher risk of developing lung cancer compared to carriers who were not smokers [29]. Rearrangements of ROS1 [30], a receptor tyrosine kinase, and anaplastic lymphoma tyrosine kinase (ALK) [31] are also recognized as molecular triggers of NSCLC and represent viable therapeutic targets.

1.1.3 Treatments for NSCLC

Surgery is recognized as the optimal treatment option for resectable tumors in patients deemed to be fit for surgical intervention that have been diagnosed with early stage I, II, or IIIA NSCLC disease [6]. However, 30-55% of patients develop recurrence of the disease [32] and approximately 70% of patients are diagnosed at later stages, specifically locally advanced or metastatic disease, due to the lack of effective screening methods [16,33]. Adjuvant chemotherapy is generally an option following surgery for patients at more advanced stages, specifically stage II and III, where cisplatin-based

chemotherapy has shown efficacy [34]. A meta-analysis evaluating chemotherapy in NSCLC patients from 52 randomized clinical trials concluded that the use of platinum-based chemotherapy following surgery showed a 5-year survival benefit compared to surgery alone [35]. For patients presenting with locally advanced or metastatic disease, platin-based combination chemotherapy is the standard of care [36,37]. A meta-analysis study evaluating various clinical trials employing platin-based chemotherapy concluded that chemotherapy improves overall survival in patients with advanced NSCLC [38]. Furthermore, this therapy, employing either cisplatin or carboplatin, is generally used as a doublet in combination with other chemotherapeutic agents, which includes docetaxel, gemcitabine, and vinorelbine [16].

Radiation therapy is another option in the case of patients diagnosed with unresectable lung cancer [39]. In a study by Wolf et al., survival following treatment with radiation therapy was higher compared to a placebo in patients with adenocarcinoma and squamous cell carcinoma, thus suggesting radiation therapy as a potentially effective treatment [40]. Several studies have suggested the combination of radiation therapy with cisplatin-based chemotherapy as a more effective therapeutic strategy for NSCLC [41,42].

There is currently a focus on targeted therapies based on alternations/biomarkers observed in a subset of patients with NSCLC [25]. These alterations include mutations in the EGFR gene and rearrangements in the ALK gene, which tend to sensitize patients to EGFR and ALK TKIs, respectively [24,31]. Despite targeted therapies showing promise, only a small subset of patients, mainly patients with adenocarcinoma, are associated with these known driver mutations [25]. Moreover, acquired resistance to TKIs has also

limited its use in a clinical setting [25]. Therefore, DNA damaging agents, such as platins, continue to be commonly employed in patients with advanced NSCLC [36].

1.2 Cisplatin

1.2.1 History of cisplatin

Cis-dichlorodiammineplatinum (II), commonly known as cisplatin, was initially synthesized by Michele Peyrone in 1844 [36]. However, it was in the 1960s that Barnett Rosenberg and his colleagues observed that platinum mesh electrodes generated cisplatin that inhibited cell division in *Escherichia coli*, which identified the potential of employing cisplatin as a chemotherapeutic agent [43,44]. Subsequently, cisplatin displayed efficacy against sarcoma and leukaemia in *in vivo* mouse models [44]. In 1978, cisplatin became the first FDA-approved platinum compound for cancer treatment against testicular and bladder cancers [45], and its use has since been expanded and is widely used as a treatment for a variety of other types of cancers, including ovarian [46], cervical [47] as well as NSCLC [38].

Cisplatin is traditionally recognized as a DNA damaging agent that enters the cell as a neutral molecule and becomes activated following the aquation of one or both of its chloride ligands [45]. This results in cisplatin becoming a positively charged electrophile that is able to covalently bind the negatively charged nucleic acids and proteins [48]. In DNA, cisplatin binds to the N7-position of its guanine bases to form mono- or bi-functional adducts [45]. This leads to the formation of inter- and intra-strand crosslinks, blocking DNA transcription and replication [45].

DNA damage results in cell cycle arrest, where the cell will try to overcome the DNA damage through the nucleotide excision repair (NER) pathway or increased tolerance of the damage [49]. However if the DNA lesions are unable to be repaired, a number of signal-transduction pathways will be activated leading the cell towards apoptosis [49]. The complete understanding of the mechanisms and pathways through which cisplatin leads to apoptosis is still not completely understood, although several pathways that have been implicated [49].

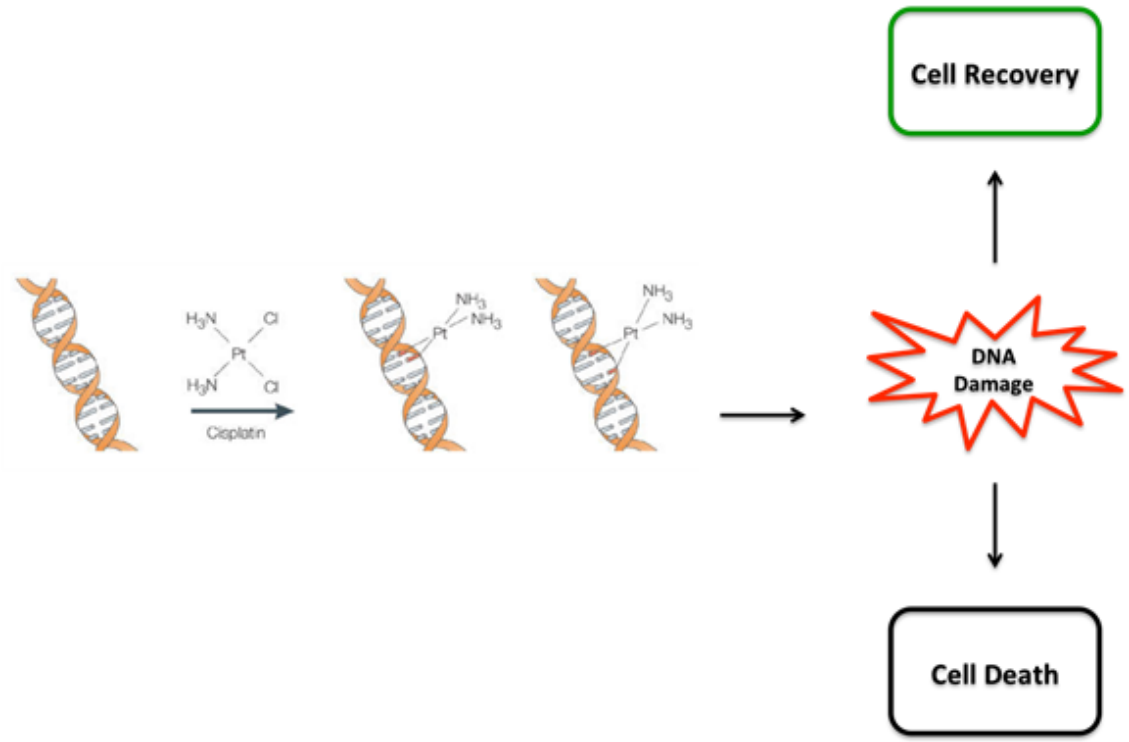

Figure 1.1. Mechanism of cisplatin-DNA adduct formation leading to DNA damage. Following its activation upon entering the cell, cisplatin forms inter- and intra-strand crosslinks with the DNA, leading to DNA damage. The cell undergoes cell cycle arrest, as well as replication and transcription inhibition, where the cell will attempt to overcome the damage and recover. However, failure to recover will ultimately lead to cell death. Adapted and modified from Wang and Lippard (2005) [50].

1.2.2 Limitations of cisplatin

As mentioned, cisplatin is a widely employed anticancer agent [36]. In fact, platins are involved in approximately 40% of all chemotherapy schedules [51]. Platin-doublet chemotherapy is considered a standard of care for patients with advanced NSCLC, however, the response rate is 17-32% for patients with NSCLC [37,52], therefore, a significant percentage of patients are being exposed to platin toxicities without receiving clinical benefit. The use and efficacy of cisplatin is restricted due to associated toxicities and resistance [36], which will each be discussed in more detail.

Toxic Side Effects

Cisplatin's cytotoxic effects are not exclusive to cancer cells; therefore it can lead to side effects in normal tissues [53]. These side effects include nausea, myelosuppression, immunosuppression, nephrotoxicity, neurotoxicity and ototoxicity [45,53]. These toxicities are dose-dependent and hence limit its potential efficacy [53]. Nephrotoxicity is considered cisplatin's main limiting side effect, as it leads to acute kidney injury (AKI) in 20-30% of patients [54]. The production of reactive oxygen species (ROS) by cisplatin-induced cytotoxicity is considered a key mechanism for this nephrotoxicity [55].

In an effort to reduce the toxic side effects observed with cisplatin, various cisplatin derivatives were developed, including carboplatin [45,56]. Carboplatin's mechanism of action is believed to be relatively similar to that of cisplatin; however, it is associated with less toxic side effects due to having a more stable leaving group, bidentate dicarboxylate [36]. Higher concentrations of carboplatin must be administered

due to its slower DNA binding rate [45]. Carboplatin does display less nephrotoxicity and neurotoxicity; however, it induces significant myelotoxicity [57]. de Castria et al. evaluated cisplatin versus carboplatin in patients with advanced NSCLC and concluded that although these agents have different toxicity profiles, no difference in overall survival (OS) was observed between the two [58]. A meta-analysis study by Ardizzoni et al. on the efficacy of cisplatin versus carboplatin based regimens in NSCLC patients observed a slightly higher response rate in patients undergoing cisplatin-based regimens [59]. Both cisplatin and carboplatin continue to be used in the clinical setting at the discretion of the physician, whose decision depends on various factors including the patient's performance and tolerance of the agent as well as the intent of the treatment [57].

Tumor Resistance

Another major obstacle for the treatment of NSCLC is the intrinsic and acquired resistance associated with cisplatin treatments [60]. Several cancers, including colorectal, lung and prostate, tend to be intrinsically resistant to cisplatin [60], while others, such as ovarian cancer, which are initially sensitive to cisplatin, tend to develop resistance over time [61]. Therefore, resistance is considered a key factor in limiting response of a wide-range of patients to cisplatin [60]. A variety of mechanisms have been associated with resistance to cisplatin as it is considered to be multi-factorial since one or a combination of these mechanisms could lead to resistance in patients [60]. Cisplatin resistance can be divided into three broad categories, which are pre-target resistance, on-target resistance and post-target resistance [60].

1) Pre-target resistance

Mechanisms that can influence the number of platin-DNA adducts formed can play a role in cisplatin resistance [60]. Reduced intracellular cisplatin accumulation is a mechanism of resistance occurring prior to the binding of cisplatin to DNA [60]. A reduction of cisplatin uptake is attributed to the transmembrane protein copper transporter I (CTR1), responsible for copper homeostasis in cells [62,63]. CTR1 has been identified as a key player in the cell's ability to uptake cisplatin as the accumulation of cisplatin in Ctr1-/- mouse embryonic fibroblasts (MEFs) was less than its wild type counterpart [63]. Additionally, Ctr1-/- MEFs were resistant to cisplatin cytotoxicity [63]. Furthermore, cisplatin exposure results in the internalization of CTR1 in ovarian cancer cells, which leads to its degradation by proteasomes, thus highlighting another potential mechanism for cisplatin resistance [64,65].

An increase in the efflux of cisplatin has also been suggested as a pre-target mechanism of cisplatin resistance [60]. The ATP-binding cassette (ABC) family of ATPases contains proteins such as multidrug resistance protein (MRP) 1, MRP2, and MRP3, which have been associated with drug resistance through increased efflux [66]. More specifically, MRP2 has been identified as the key player in this mechanism of resistance following its overexpression [67]. The overexpression of the efflux proteins copper-transporting P-type adenosine triphosphate A (ATP7A) and ATP7B have also been associated with cisplatin resistance [68,69]. Furthermore, the overexpression of ATP7B has been suggested as a potential predictor of cisplatin resistance in ovarian cancer [70].

Activated cisplatin in the cell tends to have an affinity for nucleophilic species in the cytoplasm, which includes thiol-containing molecules glutathione (GSH) and metallothioneins [60]. An increase in the levels of GSH has been observed in various cisplatin-resistant ovarian cancer cell lines [71]. The binding of cisplatin to these thiol-containing proteins limits the amount of active cisplatin that can form DNA-adducts in the nucleus [49]. Moreover, the cisplatin-GSH compound, which is catalyzed by glutathione S-transferase (GST), tends to be exported from cells via the ATP-dependent glutathione S-conjugate export (GS-X) pump (MRP2), thus further contributing to cisplatin resistance [72].

2) On-target resistance

Cisplatin resistance in cancer cell lines could also occur due to a defect in DNA-adduct recognition or an increased repair or tolerance of these adducts [60]. DNA lesions caused by cisplatin tend to be removed or repaired by the NER pathway [60]. A correlation between increased NER proficiency and cisplatin resistance has been shown in several models [73,74]. A key protein in the NER pathway is the excision repair cross-complementing-1 (ERCC1) protein, which is an endonuclease that heterodimerizes with xeroderma pigmentosum complementation group F (XPF) in order to incise DNA on the 5' section of cisplatin adducts [45]. The expression of ERCC1 has been correlated with increase cisplatin resistance and a decrease in survival in various cancer models including NSCLC [75], ovarian [73], as well as head and neck [76]. Interestingly, testicular cancers, which are known to be highly sensitive to cisplatin treatment, with 80% of patients becoming cured following treatment, have been shown to be deficient in ERCC1-XPF [77].

The DNA mismatch repair (MMR) pathway is responsible for the repair of errors, including incorrect base insertions and deletions, during DNA replication [78]. However, in the case of DNA adducts, it is able to detect them but fails to repair, which leads to the induction of apoptosis by activating the tyrosine kinase v-abl Abelson murine leukaemia viral oncogene homologue (c-Abl) as well as the pro-apoptosis protein p73 [79]. Therefore, a defect in the MMR pathway could lead to cisplatin resistance [49].

As mentioned, an increased tolerance to the cisplatin-DNA adducts could also be a factor for cisplatin resistance [60]. Translesion synthesis (TLS) is a mechanism that plays a role in this tolerance [80]. This mechanism entails the ability of a number of specialized DNA polymerases, known as TLS polymerases, bypassing DNA lesions [80]. In the case of cisplatin-GG adducts, the TLS polymerases pol η (POLH) and pol ζ (REV3 and REV7) have been associated with its bypassing [80]. Additionally, the DNA polymerase β (pol β) has also been shown to be involved in bypassing cisplatin adducts, thus contributing to the development of cisplatin resistance [80,81].

3) Post-target resistance

Post-target resistance to cisplatin can result from defects that occur in the signalling pathways that induce apoptosis following DNA damage [60]. Cisplatin-induced apoptosis can occur through the intrinsic apoptotic pathway or the extrinsic apoptotic pathway [36]. There are several proteins that play a role in these pathways, which include p53, mitogen-activated protein kinase (MAPK) signalling cascades as well as the pro-apoptotic B-cell lymphoma (Bcl-2) family of proteins [82,83,84]. Caspases are essential in both the intrinsic and extrinsic apoptotic pathways, and their defects have been associated with cisplatin resistance [36].

P53 is a widely recognized tumor suppressor protein that plays a role in number of cellular pathways, including the DNA damage response (DDR) [82]. A deficiency in p53 has been shown to contribute to cisplatin resistance in a number of cancer cell lines [60]. For example, ovarian cancer patients with a wild type p53 are more responsive to cisplatin compared to patients with a p53 mutation [85]. Additionally, testicular cancers, which tend to be extremely sensitive to cisplatin [86], rarely contain a p53 mutation [87]. However, there have been studies that report no correlation between p53 status and cisplatin resistance [88,89]. This could be due to other factors that could potentially be playing a role alongside p53, which includes other genetic alternations and cellular context, including type of cell and signalling pathways [90].

The MAPK signalling cascades are known to play an important role in transducing extracellular signals into cellular responses [91]. The MAPK family consists of three protein kinases, which are extracellular signal-regulated kinase (ERK), c-Jun N-terminal kinases/stress-activated protein kinases (JNK/SAPK) and p38 [91]. These kinases can be activated by external stimuli, which is transduced to cellular responses by phosphorylation [91]. The MAPK cascades have been shown to play a role in cisplatin cytotoxicity [79,83]. The induction of the p38 pathway by cisplatin leads to apoptosis, while the induction of the JNK and ERK pathways by cisplatin could induce cell survival or apoptosis [83]. Furthermore, specifically inhibiting the activity of p38 can lead to an increase in cisplatin resistance [92,93].

The increase in the expression of anti-apoptotic proteins, such as Bcl-2 and Bcl-XL, has also been associated with cisplatin resistance in a number of cancers, including ovarian and NSCLC [94,95]. The inhibitor of apoptosis (IAP) family of proteins are

responsible for inhibiting caspases, which inhibits cell death [80]. In this family, the increased expression of X-linked inhibitor of apoptosis protein (XIAP) has been associated with cisplatin resistance in ovarian cancer cell lines [80]. The overexpression of another member the IAP family, known as survivin, has also been associated with cisplatin resistance in various cancer cell lines [80].

1.2.3 Cisplatin-induced stress pathways

Cisplatin is widely recognized as a DNA damaging chemotherapeutic agent, and as previously mentioned, functions by forming adducts with the cellular DNA, leading to DNA damage, which the cell will try to repair [45,49]. A key player in the DNA repair mechanism in response to DNA damage is the NER [60]. Thus, once DNA damage has occurred, the cell undergoes cell cycle arrest, which enables the NER complex to recognize and excise the DNA lesion, followed by DNA synthesis to reinstate genomic integrity [60]. However, if the DNA damage is sustained and thus causing the DNA repair to remain incomplete, the cells will activate signalling pathways that have the potential to lead the cell towards apoptosis [49]. The inductions of various pathways have been recognized following cisplatin treatment, including, but not limited to, the DDR [96], MAPK cascades [83] and the induction of ROS by oxidative stress [84]. These pathways have been recognized to play a role in stress responses as well as growth and differentiation [45].

1) DNA damage response

The formation of cisplatin-DNA adducts that leads to double-stranded breaks (DSB) activates a DNA damage response [96]. The role of the DDR in the cell is to maintain

genomic integrity through efficient repair of DNA damage [97]. Activation of the DDR initially results in cell cycle arrest for DNA repair to occur [97]. However, sustained DNA damage will eventually trigger cellular apoptosis [49]. Two key upstream regulators involved in the DDR are the protein kinases Ataxia telangiectasia mutated (ATM) and the ATM and Rad-3 related (ATR) [96]. ATM tends to be activated in response to DSBs, leading to the activation of histone H2AX, while ATR tends to be activated upon replication stress and single strand breaks [98]. The activation of ATM and ATR leads to the phosphorylation of other kinases, including checkpoint kinase (Chk) 1 and Chk2, which leads to the induction of p53, a key protein in DDR response [96]. Generally, low levels of p53 are expressed in cells, however, upon various stimuli, including DDR activation, p53 levels are increased [99]. The activation of p53 leads to the induction of p21, a cyclin dependent kinase inhibitor (CDKI), which leads to G1/S arrest [96]. When the DNA damage is deemed irreparable, apoptosis will be favoured, where p53 will induce the translocation of the pro-apoptotic protein Bcl-2-associated X (BAX) from the cytosol to the mitochondria, where the activation of the caspase 9-caspase 3 pathway will induce apoptosis [49]. Furthermore, p53 mutations commonly result in the inhibition of tumor cell apoptosis, however, apoptosis can also be induced in a p53-independent manner [100]. Another key player in the process is the anti-apoptotic Bcl-2 protein, which is repressed in this event [49]. Ultimately, it is the Bax:Bcl-2 ratio that is a determinant in the occurrence of apoptosis [49].

2) MAPK cascades

The MAPK signalling pathway has been shown to play a role in cellular proliferation, differentiation, development, as well as inflammatory responses and apoptosis [91].

Previous studies, including our own, have demonstrated the activation of all three MAPK kinases following cisplatin treatment in cancer cells [83,101]. The activation of ERK has been suggested as highly important as it has been associated with the phosphorylation of p53 [102], while other studies have highlighted p38 [92] and JNK [103], as contributing to cisplatin-induced apoptosis. It is however important to note that although these MAPK kinases have a role in inducing apoptosis following cisplatin treatment, they have also been implicated in contributing to cisplatin-resistance [83,104]. This has been attributed to the extent of DNA damage induced by cisplatin and the difference in cellular context [49].

3) Oxidative stress and ROS formation

Apart from DNA damage, oxidative stress is known to play a role in cisplatin cytotoxicity through the induction of ROS [84]. The formation of ROS is dependent on the cisplatin's concentration and length of exposure [84]. Cisplatin leads to cell death by inducing DNA damage at low doses, while inducing ROS formation, specifically superoxide, at higher doses in the colon carcinoma cell line HCT116 and melanoma cells 224 [105]. The presence of superoxide scavengers was shown to inhibit cell death [105]. The mitochondria is believed to play a role as it is responsible for energy production through oxidative phosphorylation and a source of ROS formation in cells [106]. Other than forming DNA adducts in the nucleus, cisplatin is also known to form adducts with mitochondrial DNA, which induces mitochondria-dependent ROS formation, and enhances cisplatin's cytotoxicity [106]. The impaired mitochondrial oxidative stress is believed to result in impaired protein synthesis, altered mitochondrial membrane potential (MMP), and defective energy metabolism [106,107]. Furthermore, ROS

formation has also been associated with the activation of the MAPK pathway [108] as well as the Integrated Stress Response (ISR) [109], which plays a role in maintaining cellular homeostasis in response to stressful stimuli [110].

1.3 Activating Transcription Factor 3 (ATF3)

1.3.1 Cellular stress response and ATF3

Cellular stress response is generally recognized as a protective mechanism against potentially threatening stimuli, including injury, hypoxia and DNA damage [111]. A lack of response to stress can lead to the development of cancer [111]. Activating transcription factor (ATF) 3 is a member of the ATF/cyclic AMP response element binding (ATF/CREB) family of basic region-leucine zipper (bZip) transcription factors, which were originally identified due to their ability to bind to the consensus ATF/CRE site 'TGACGTCA' [112]. The ATF3 gene is located on chromosome 1q32.3 and its protein consists of 181 amino acids [112] and has a molecular weight of 22 kDa [113]. The human ATF3 mRNA consists of four exons, which are distributed over 15 kilobases [112]. These exons are referred to as exons A, B, C and E [112]. Exon A contains the 5'-untranslated region, while exon B contains the N-terminal as well as the initiation codon (AUG) [112]. Exon C mainly contains the basic region, while exon E contains the ZIP domain and the 3'-untranslated region [112]. Furthermore, an alternatively spliced isoform of ATF3, known as ATF3ΔZip, also exists and includes an exon between exon C and E, referred to as exon D, which contains an in-frame termination codon [112,113]. This results in a truncated protein, as it no longer contains the leucine zipper region at the C terminus, therefore preventing it from binding to the ATF/CRE motif [112,113]. ATF3ΔZip was determined to play a role in the expression of target genes by

sequestering co-inhibitory factors from the promoters [113]. Furthermore, another alternatively spliced isoform, known as ATF3ΔZip2, was identified and suggested to play a role in the regulation of gene expression upon stress stimuli [114].

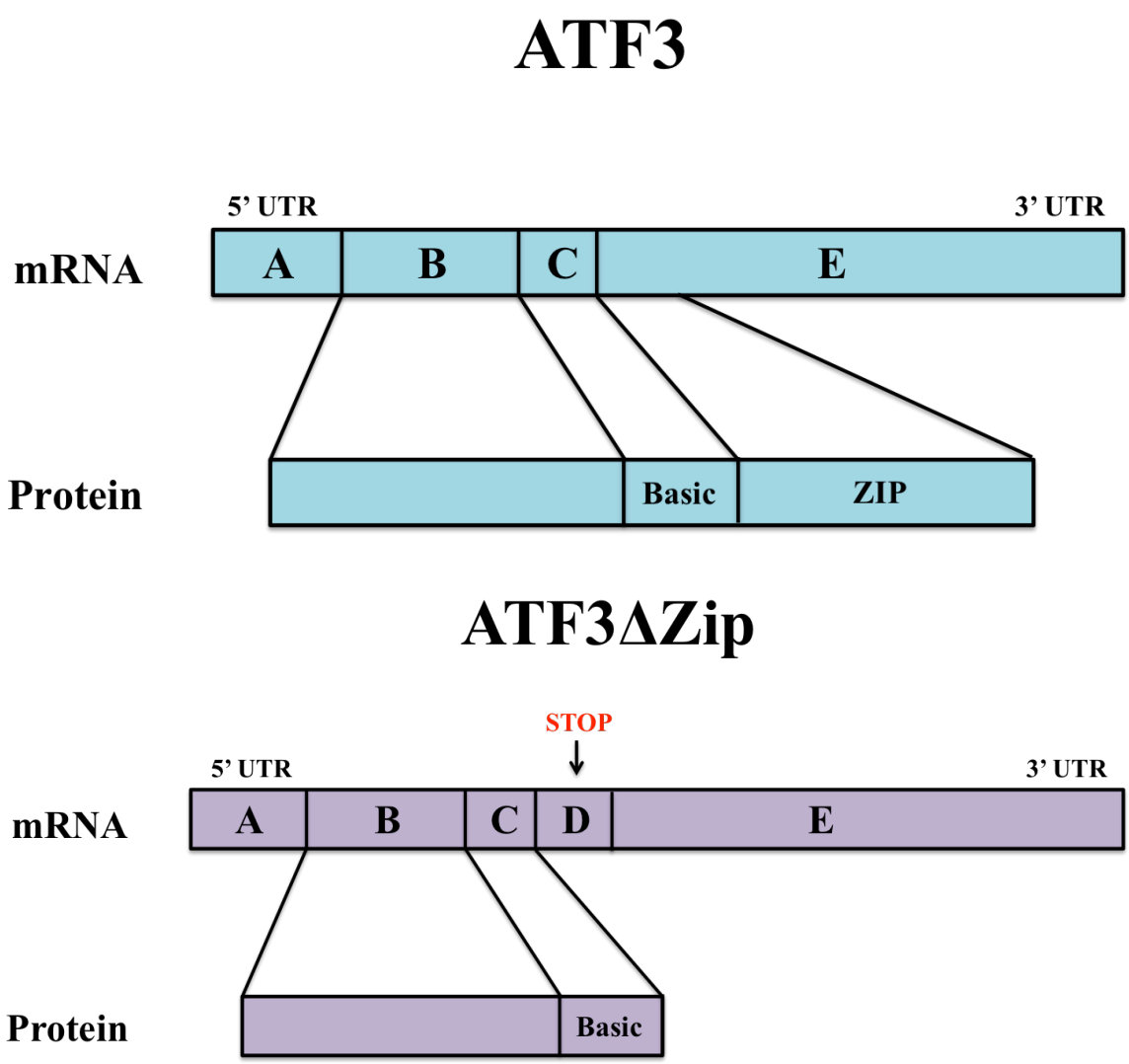

Figure 1.2. ATF3 and ATF3ΔZip exon organization. The ATF3 mRNA contains four exons, A, B, C and E, which result in a full length ATF3 protein. The ATF3ΔZip mRNA contains exons A, B, C, D and E, where exon D contains a stop codon that leads to the formation of a truncated protein lacking the leucine zipper region. Adapted and modified by Liang et al. (1996) [112].

As a member of the activating protein 1 (AP-1) family of transcription factors, ATF3 can homodimerize or selectively heterodimerize with other proteins of this family, which include ATF2, c-Jun, Jun B and Jun D, through the leucine zipper region [115,116]. It has been shown that when ATF3 homodimerizes, it acts as a transcriptional repressor, however, it can activate or repress transcription as a heterodimer [117]. The promoter and cellular contexts as well as the availability of binding partners are important determinants as to whether the dimers will act as transcriptional activators or repressors [113,117]. As an example, the ATF3/c-Jun, ATF3/JunD and ATF3/JunB heterodimers activate promoters with ATF/CRE binding sites, however, the ATF3/JunB heterodimer represses promoters with AP-1 binding sites [117,118].

1.3.2 ATF3 as a stress-inducible gene

In most cell lines and tissues, the basal expression level of ATF3 is low, however, ATF3 can be induced by a variety of different stimuli, thus earning its title as a stress-inducible gene [117,119]. ATF3 induction was initially observed in tissues following physiological stress, which included liver injuries and ischemia [119]. ATF3 is also induced by other stress stimuli such as genotoxic agents, including ionizing radiation (IR), ultraviolet light (UV) [120] and doxorubicin [121]. Endoplasmic reticulum (ER) stressors [122], oxidative stress [123] and proteasome inhibition [124] have also been identified as ATF3 inducers. Furthermore, our laboratory has also identified cisplatin as an inducer of ATF3 as well as mevalonate pathway inhibitors [125] and histone deacetylase inhibitors (HDACi) [126].

1.3.3 Mechanisms involved in ATF3 induction

Depending on the strength of the stressor stimuli as well as cellular context, the induction of ATF3 will lead to the activation of target genes through an array of signalling pathways that can either help alleviate the stress, or, in the case the stress can not be overcome, lead to apoptosis by inducing pro-apoptotic factors, such as C/EBP homologous protein, also known as growth arrest DNA damage inducible gene 153 (GADD153) [117,119,120]. Pathways that have been associated with the induction of ATF3 following stress stimuli include, the DDR, specifically p53 [111], the MAPK cascades [101,127] and the ISR pathway [125,126,128].

The DDR plays an important role in regards to ATF3 induction as there is a p53 binding site present on the ATF3 promoter and efficient ATF3 induction is often dependent on an intact p53 allele [129]. Following genotoxic induced DNA damage, it has been reported that ATF3 interacts with p53 to increase its stability, thus preventing p53 from proteasomal degradation [111]. A role for ATF3 has also been shown in the suppression of the oncogenic activities of mutant p53, which is interesting as both NSCLC cell lines used throughout this thesis, specifically Calu6 and H23, contain p53 mutations [130]. Therefore, these suggest that ATF3 plays a role in regulating p53 tumor suppressor functions. Additionally, the loss of ATF3 has been shown to result in defective p53 induction following DNA damage [131].

The ISR pathway is involved in cellular stress response in eukaryotes [110]. This pathway involves the phosphorylation of eukaryotic translation initiation factor 2 alpha (elF2α), which leads to global protein synthesis inhibition and the activation of a number

of genes, including ATF4, and subsequently ATF3 [128]. The pro-apoptotic factor CHOP/GADD153 is downstream of ATF3 in this pathway [122].

The induction of ATF3 can also occur through the MAPK pathway [101,127]. As previously mentioned, the MAPK pathway is induced by cisplatin, however, our laboratory has previously shown that the activation of this pathway leads to ATF3 induction [83,101]. Moreover, ATF3 was shown to be a key regulator in cisplatin cytotoxicity [101]. In addition to cisplatin, there are other stimuli that induce ATF3 through the MAPK pathway, which include the protein synthesis inhibitor anisomycin, which induces ATF3 through the p38 pathway [127], and the non-steroidal anti-inflammatory drug tolfenamic acid, which induces all three MAPK components, leading to the phosphorylation of ATF2 and subsequent induction of ATF3 [132].

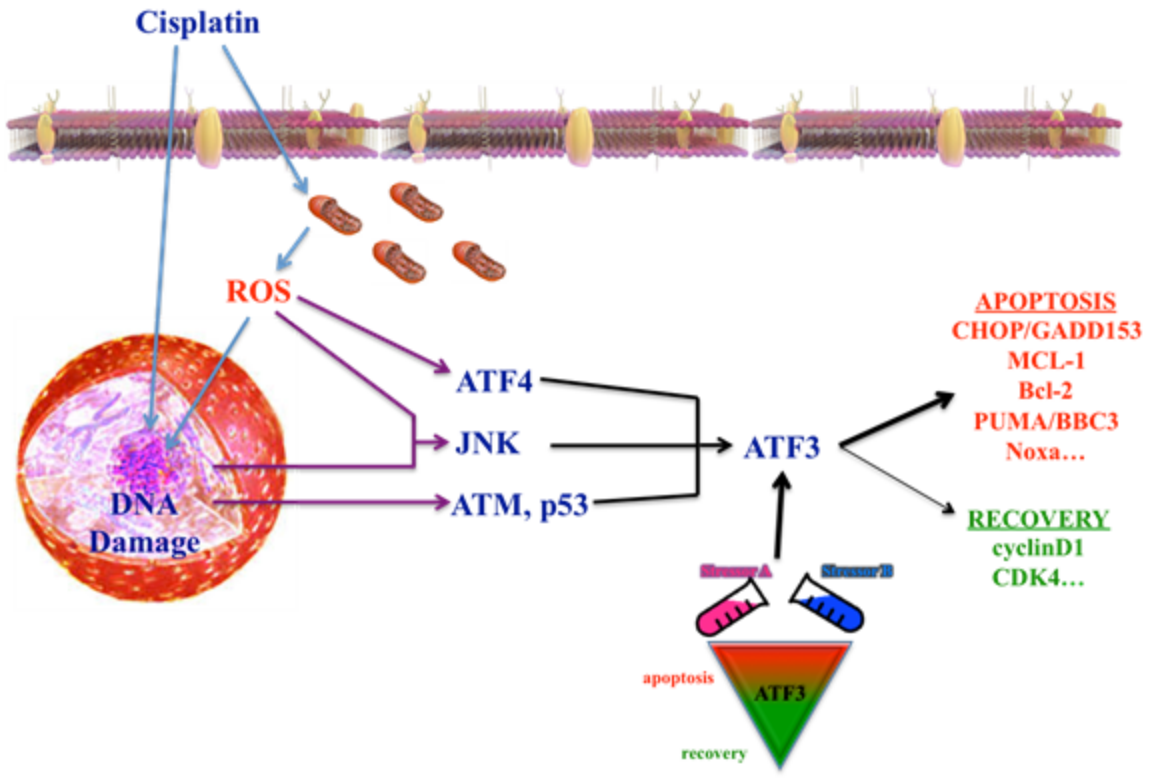

Figure 1.3. Schematic model of various pathways through which cisplatin has been shown to induce ATF3 expression. Cisplatin can lead to DNA damage and ROS production, and induce various pathways, including the ISR, MAPK, as well as components of the DDR, which can lead to the induction of ATF3 and consequently its downstream targets that play a role in either apoptosis or cell recovery [84,122,133–136].

1.3.4 ATF3's role in cancer

In the context of cancer, it has been suggested that ATF3 has a dichotomous role as it has been shown to play a role in the proliferation or apoptosis of cancer cells [137,138]. An example of this dichotomous role was observed where overexpression of ATF3 induced apoptosis in the untransformed MCF10A mammary epithelial cells, while protecting the aggressive breast cancer cell line MCF10CA1a and enhancing its motility [137]. ATF3 also binds to the cyclin D1 promoter and represses its transcription, resulting in cell cycle arrest and apoptosis in Ras-mediated tumorigenesis [135]. Additionally, the overexpression of ATF3 displayed an antitumorigenic effect in *in vitro* colorectal cancer cells and *in vivo* mouse xenograft model [139]. Although several studies support ATF3's role in apoptosis, an oncogenic role for ATF3 has also been reported. A study evaluating ATF3 expression levels in human lung cancer tissues correlated higher ATF3 expression with advanced tumor grade and metastasis as well as a shorter overall survival [140]. Additionally, the tumor metastasis suppressor gene Drg-1 has been shown to downregulate the transcription of ATF3 in prostate cancer cell lines [141]. The overexpression of ATF3 in these cells promoted invasion *in vitro* and enhanced metastasis in an *in vivo* mouse model [141].

The difference observed in the role of ATF3 could be contributed to cellular context and state of malignancy in the studies done, however, the role of ATF3 in both cellular proliferation and apoptosis warrants further studies.

1.3.5 Previous work from our laboratory: Evaluating the induction of ATF3 by cisplatin

The induction of ATF3 by cisplatin was previously demonstrated in our laboratory [101]. This study evaluated a number of pathways that have previously been identified to induce ATF3 and determined that cisplatin induces ATF3 through a MAPK-dependent pathway [101]. All three components of the MAPK pathways were shown to play a role in the induction of ATF3 as the inhibition of the ERK, p38 and JNK pathways inhibited the induction of ATF3 following cisplatin treatment [101]. Additionally, our lab used two cisplatin-resistant cell lines derived from the parental NSCLC cell lines Calu6 and H23, designated as Calu6cisR1 and H23cisR1 [104]. Both Calu6 and H23 are adenocarcinoma cell lines with genetic mutations in p53 and KRAS, which are commonly observed in this tumor type [142, 143]. RNA-seq transcriptome analysis was performed in order to identify genes that are differentially induced between the parental Calu6 and H23, and their cisplatin-resistant counterparts, following treatment with 2μg/mL cisplatin for 24 hours (Figure 1.4A). ATF3 was significantly induced in the parental cell lines but not in their cisplatin-resistant counterparts (Figure 1.4B). The induction of ATF3 was abrogated at the protein and mRNA level in the cisplatin-resistant cell lines (Figure 1.4C and D), which was attributed to a defect in the JNK pathway signalling, further highlighting the role of the MAPK pathway is cisplatin cytotoxicity and resistance [104].

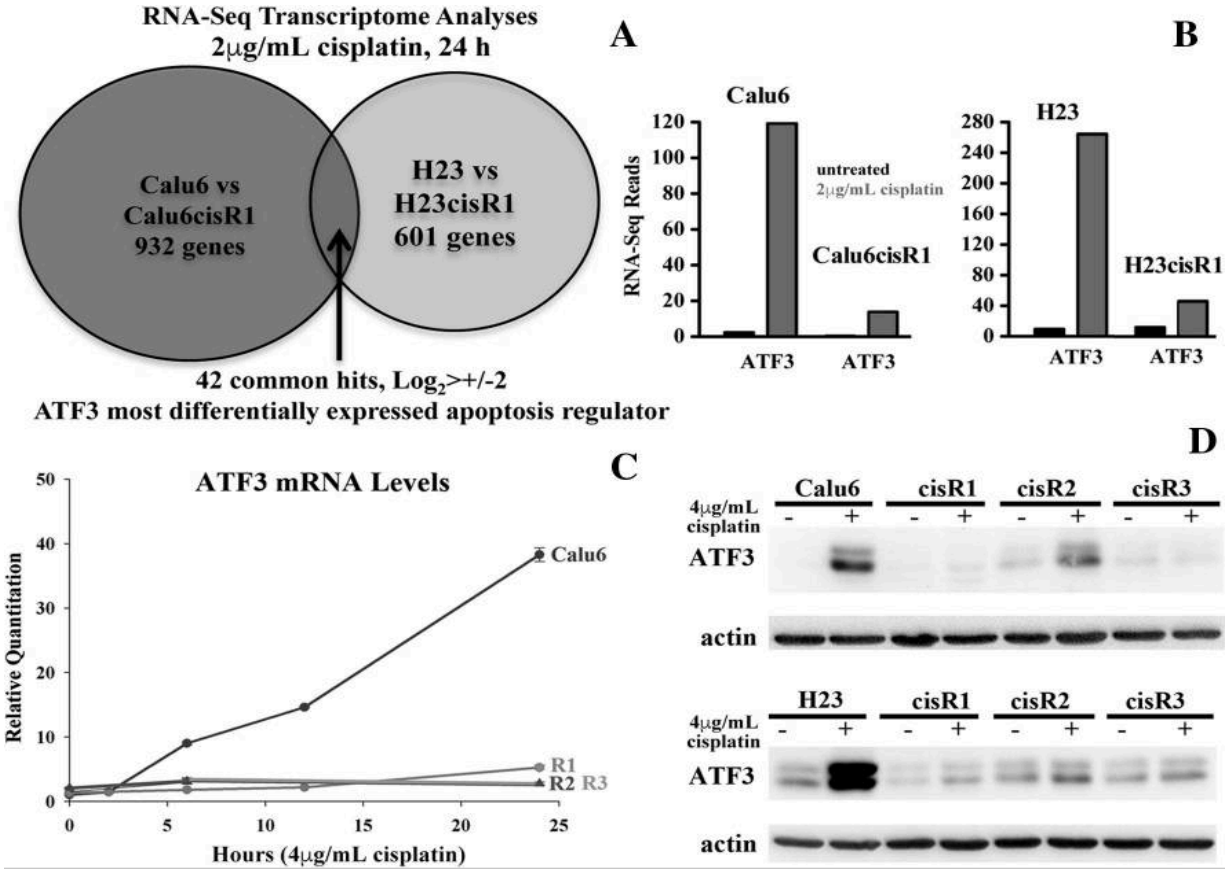

Figure 1.4. Differential regulation of ATF3 between parental and cisplatin-resistant NSCLC cell lines. A) RNA-seq analysis of Calu6 and H23 and their cisplatin-resistant sub-lines, Calu6cisR1 and H23cisR1, following treatment with 2μg/mL cisplatin for 24 hours. **B)** ATF3 was identified as a differentially expressed gene between the parental and cisR1 cells following cisplatin treatment (2μg/mL cisplatin for 24 hours). **C)** RT-qPCR evaluation of ATF3 mRNA levels in Calu6 and the three cisR1 sub-lines following treatment with 4μg/mL cisplatin for up to 24 hours. **D)** Western blot analysis of ATF3 expression in the parental Calu6 and H23 and their cisR1 sub-lines following treatment with 4μg/mL cisplatin for 24 hours. Data in this figure were obtained by Jair Bar [104].

Moreover, platin regimens tend to consist of the combination of platins with other agents in order to increase the efficacy of the treatment [16]. Previous works in our laboratory have investigated the combination of cisplatin with other ATF3 inducers, including HDACi M344 [126] and disulfiram, a drug commonly used for alcohol aversion therapy [144]. Both combinations showed enhanced cisplatin cytotoxicity as well as ATF3 protein induction [126,144]. Current agents used in combination with platins in the clinical setting have been determined empirically [145]. However, identifying more rational combination based therapies is important to overcome the toxicities and resistance associated with the current regimens.

Our laboratory employed a chemical library of 1200 FDA approved compounds to identify agents that can enhance cisplatin cytotoxicity using the Calu6 NSCLC cell line (Table 1a). This library was also employed to identify agents whose cytotoxicity was ATF3 dependent by comparing responses in wild type MEFs compared to ATF3-deficient (ATF3-/-) MEFS (Table 1b). Two agents that were identified in both screens are vorinostat and topotecan (Table 1). Vorinostat, also known as suberoylanilide hydroxamic acid (SAHA), is a histone deacetylase (HDAC) inhibitor that targets class I and II HDACs [146]. Histone deacetylases are responsible for catalyzing the removal of acetyl groups from histones, which results in transcriptional repression [147]. Vorinostat inhibits these enzymes by binding to the zinc atom that is located on the catalytic site of the HDACs, resulting in an accumulation of acetylated proteins, including histones [146]. HDAC inhibitors have anticancer activity by inducing apoptosis and cell cycle arrest [148,149] and approved for the treatment of cutaneous T cell lymphoma [150]. Topotecan, also known as Hycamtin, is a topoisomerase I inhibitor that has also been

FDA approved as a chemotherapeutic agent for a variety of cancers [151,152]. Topotecan's interference between the topoisomerase I enzyme and DNA results in double strand breaks, eventually leading the cell to apoptosis [152]. In this study, we investigated the role of vorinostat and topotecan as inducers of ATF3 and their effects on cisplatin induced cytotoxicity in NSCLC cells.

a. Calu6: 1200 FDA compound screen (1µM dose) + 0.4µg/mL cisplatin

Anthracyclins	Topoisomerase I Inhibitors	Microtubule Polymerization	Antimetabolites	Metabolic Stressors
doxorubicin	campothecin	docetaxel	gemcitabine	vorinostat
daunorubicin	topotecan	nocodazole	floxuridine	antimycin
mitoxantrone			azacytidine	

b. ATF3+/+ vs. ATF3-/- 1200 FDA compound screen (5µM dose)

NSAIDS	Topoisomerase I Inhibitors	Antimetabolites	Metabolic Stressors	Antibiotics
zomepirac	topotecan	zalcitabine	atovaquone	cefmetazole
piroxicam	etoposide	azaguanine-8	vorinostat	minocycline
	podophyllotoxin	mercaptopurine	monensin	quinacrine
		thioguanosine	fluvastatin	alexidine
		trifluridine	nafronyl oxalate	
			isosorbide	

Table 1.1. Compounds obtained as hits by employing a chemical library screen of 1200 FDA approved compounds. **a)** Calu6 cell line was used in order to identify compounds that enhanced cisplatin sensitivity (24 hours library treatment + 48 hours with cisplatin for a total of 72 hours) and **b)** wild type and ATF3-/- MEFS were used in order to identify differential sensitivity (48 hour treatment). Compounds in red represent compounds of interest for this study. Done by Stephanie Reid and Shaad Hasim.

1.4 Rationale

Platin-based combination chemotherapy is the standard of care for treatment of patients with advanced NSCLC [36]. However, cisplatin associated toxicities and resistance act as barriers to its efficacy [36]. Our laboratory has identified ATF3 as a mediator of cisplatin cytotoxicity [101] and further highlighted its potential role in mediating cisplatin resistance in NSCLC [104]. Furthermore, the combination of cisplatin with other ATF3 inducers, such as M344 and disulfiram, enhance cisplatin cytotoxicity [126,144]. We further identified vorinostat and topotecan as hits in a strategically performed library screen that demonstrated their roles as both enhancers of cisplatin cytotoxicity as well as agents whose cytotoxicity is dependent on ATF3. Therefore, their combination with cisplatin could potentially lead to enhanced and sustained induction of ATF3 pushing cells towards apoptosis. The MAPK pathway has been highlighted in the induction of cisplatin cytotoxicity [83,101], however, other pathways, such as DDR and ROS, will also be evaluated to further understand the mechanisms underlying cisplatin, vorinostat and topotecan cytotoxicity.

1.5 Hypothesis and Objectives

Hypothesis

Enhanced and sustained induction of ATF3 through the combination of platins and other ATF3 inducers will result in synergistic or enhanced anti-cancer activity in NSCLC.

Objectives

1. To establish ATF3 as a therapeutic target in NSCLC through the identification and combination of novel ATF3 inducers with platins
    a. Evaluate ATF3 as a therapeutic target in NSCLC
    b. Combining novel ATF3 inducers with platins as a therapeutic approach
2. To evaluate ATF3 expression in human NSCLC *ex vivo* samples in order to further highlight its clinical relevance

Chapter 2: Materials and Methods

2.1 Tissue Culture

The human tumor-derived NSCLC cell lines Calu6 and NCI-H23 (H23) were obtained from the American Type Culture Collection (ATCC) (Rockville, MD, USA). The wild type and ATF3 deficient (ATF3-/-) MEFs were kindly provided by Dr. T. Hai (Ohio State University, OH, USA). The cisplatin-resistant Calu6 and H23 sub-lines were previously established by treating the parental cell lines with 2μg/mL cisplatin until approximately 10^{-6} cells remained, from which single cells were isolated and grown [104]. All cell lines were maintained in Dulbecco's Modified Eagle's Medium (DMEM) (Media Services, Ottawa Regional Cancer Centre, Ottawa, ON, Canada) supplemented with 10% fetal bovine serum (FBS) (Medicorp, Montreal, QC, Canada) and 100μg/mL penicillin-streptomycin (Sigma-Aldrich, St Louis, MO, USA). Additionally, the media for the MEFs was supplemented with L-Glutamine (Sigma, St Louis, MI, USA). Incubation of the cells occurred at 37°C and 5% CO2. Passaging of the cells involved washing with Dulbecco's Phosphate Buffered Saline (PBS) (Cellgro, Manassas, VA, USA) and detached using Trypsin EDTA 1x (Cellgro, Manassas, VA, USA). Cell counts were performed using a Vi-Cell XR Cell Viability Analyzer (Beckman Coulter, CA, USA).

2.2 Drugs and Inhibitors

Cisplatin, carboplatin, docetaxel, doxorubicin and topotecan were provided by the pharmacy at the Ottawa Hospital Cancer Centre (Ottawa, ON, CAN). Vorinostat was purchased from Calbiochem (Gibbstown, NJ, USA) and suspended to 10mM in dimethyl

sulfoxide (DMSO). GGTI-298 was purchased from Sigma-Aldrich (St Louis, MO, USA) and suspended to 10mM in DMSO. Lovastatin was purchased from Apotex (Toronto, ON, Canada) and suspended to 10mM in ethanol. Thapsigargin was purchased from Sigma-Aldrich (St Louis, MO, USA) and suspended to 1mM. The chemical inhibitors for JNK (SP600125) and ATM (KU55933) were purchased from Selleck Chem (Houston, TX, USA).

2.3 3-(4,5-Dimethylthiazol-2-yl)-2,5-Diphenyltetrazolium Bromide (MTT) Assay

Cells were seeded in 96-well flat-bottom plates (Costar, Corning, NY, USA) at densities previously optimized for each cell line and time points in 75 or 50 µL per well for single and combination treatments, respectively. Once seeded, the cells were incubated overnight to allow for attachment and recovery. For single drug treatments, cells were treated with increasing concentrations of cisplatin, carboplatin, docetaxel, vorinostat and topotecan for 48 or 72 hours. For combination drug treatments, cells were pre-treated with vorinostat or topotecan for 24 hours, followed by treatment with increasing concentrations of cisplatin for another 48 hours, for a total of 72 hours. The final volume for all treatments was 150µL. Following treatment, 42µL of a 5mg/mL MTT tetrazolium substrate solution (Sigma-Aldrich, St Louis, MO, USA) prepared in PBS was added to each well for 2 hours and incubated at 37°C and 5% CO2. Following that, 84µL of a solution of 0.01N HCl in 10% SDS was added to each well and incubated overnight at 37°C and 5% CO2. The absorbance was measured at 570nm with a Synergy Mx Monochromator-Based Multi-Mode Microplate Reader using the Gen5 software (BioTek, Winooski, VT, USA)

2.4 Western blot analysis

Cells were seeded in 6-well flat bottom plates (Costar, Corning, NY, USA) at a density of 600 000 cells/well. After a treatment of 24 or 48 hours, media was aspirated and the cells were washed with cold PBS. RIPA buffer (50 mM Tris-CL pH 7.5, 150 mM sodium chloride, 1 mM EDTA, 1% Triton-X-100, 0.25% sodium deoxycholate, 0.1% SDS) containing 1x Protease Inhibitor Cocktail was used for cell lysis. Protein quantification was performed using the Pierce BCA Protein Assay Kit (Pierce, Rockford, IL, USA) and the absorbance was read at 562 nm with a Synergy Mx Monochromator-Based Multi-Mode Microplate Reader using the Gen5 software (BioTek, Winooski, VT, USA). Protein samples were separated using 10-12% SDS polyacrylamide gels and transferred onto Immobilon-P PVDF membranes (Millipore, Billerica, MA, USA). Membranes were blocked with 5% milk in Tris-buffered saline containing 0.1% Tween-20 (TBS-T) for 1 hour and incubated with a primary antibody dilution in 5% milk in TBS-T overnight at 4°C.

The primary antibodies used are: rabbit anti-ATF3 (C-19) (1:500, Santa Cruz Biotechnology, Santa Cruz, CA, USA), rabbit anti-PARP (1:1000, Cell Signaling Technology, Lake Placid, NY, USA), rabbit anti-c-Jun (1:1000, Cell Signaling Technology, Lake Placid, NY, USA), rabbit anti-phospho-c-Jun (Ser73) (1:1000, Cell Signaling Technology, Lake Placid, NY, USA), mouse anti-phospho-Histone H2A.X (Ser139) (Millipore, MA, USA) and mouse anti-actin (1:10,000, Sigma-Aldrich, St. Louis, MO, USA).

The following day, the membranes were washed three times with TBS-T and incubated at room temperature for 1 hour with the appropriate horseradish peroxidase

(HRP)-labeled secondary antibody (1:3000 anti-mouse, 1:3000 anti-rabbit, Jackson ImmunoResearch, West Grove, PA, USA) in 5% milk in TBS-T. Protein bands were visualized using the Clarity Western ECL Subsrate (BioRad, Saint-Laurent, QC, Canada) and developed using the Syngene Bio-Imaging System (Syngene, Frederick, MD, USA).

2.5 *Ex vivo* tissue processing

Patient lung tumor and normal adjacent lung tissue were collected after surgical resection (lobectomy) (Ottawa Hospital Research Ethics Board; Protocol # 20120559-01H). The tissues were cored into smaller pieces (approximately 2x2x1 mm) using a sterile biopsy punch. Tumor cores were randomly distributed (3 cores/well) in a 24-well flat bottom plate (Costar, Corning, NY, USA) containing 1mL of DMEM (Media Services, Ottawa Regional Cancer Centre, Ottawa, ON, Canada) supplemented with 10% FBS (Medicorp, Montreal, QC, Canada). Treatments were performed in triplicate for 48 hours. After treatment, the cores were transferred into 1.5 mL tubes and snap frozen in liquid nitrogen and stored at -80°C.

2.6 RNA Extraction and RT-PCR for *ex vivo* tissue

For each sample, 0.5 mL of trizol was added in the 1.5mL tube and the tissues were homogenized using a PowerGen 125 tissue homogenizer (Fisher Scientific, Hampton, NH, USA) and incubated at room temperature for 10 minutes. 100µL of chloroform was added to each sample and samples were vortexed for 20 seconds and incubated at room temperature for 3 minutes. The samples were then centrifuged at 14 500 rpm for 15 minutes at 4°C and the clear aqueous phase was transferred to a new 1.5 mL Eppendorf tube. 250µL of isopropanol was added to precipitate RNA and incubated

at room temperature for 20 minutes. The samples were then centrifuged at 14 500 rpm for 15 minutes at 4°C. The liquid was removed and the pellet was washed with 1mL of 75% ethanol and centrifuged for 10 minutes at 10 000 rpm at 4°C. The ethanol was then removed and pellets were left to dry for 10 minutes. The pellets were then dissolved in 40µL of RNAase free water. RNA concentrations were measured on a Take3 Micro-Volume plate with a Synergy Mx Monochromator-Based Multi-Mode Microplate Reader using the Gen5 software (BioTek, Winooski, VT, USA).

Total RNA (0.5µg) was reverse transcribed to complementary DNA (cDNA) using a High Capacity cDNA reverse transcription kit (Applied Biosystems, Foster City, CA, USA) in an ABI Thermal Cycler (Applied Biosystems, Foster City, CA, USA), following the manufacturer's protocol. In order to detect amplification, quantitative real-time polymerase chain reaction (RT-qPCR) was performed using the Applied Biosystems AB 7500 Real-Time PCR System (Applied Biosystems, Foster City, CA, USA). A total volume of 20µL was used, consisting of 4uL of synthesized cDNA, 1µL TaqMan Gene Expression Assay Primer/Probe (20x) (Applied Biosystems, ATF3, HS00231069), 5µL of RNase free water and 10µL of TaqMan Universal PCR Master Mix (2x) (Applied Biosystems, 4303337). The housekeeping gene that was used as the endogenous control was human GAPDH (20x) (Applied Biosystems, HS4333764-F).

2.7 Statistical Analysis

The graphical data was plotted using GraphPad Prism software (Graphpad, San Diego, CA, USA). A two-way ANOVA using a Bonferroni multiple comparison test was employed to determine significance regarding MTT cell viability curves. In all cases,

*=$p<0.05$, **= $p<0.01$ and *** = $p<0.001$ indicate significance. The CalcuSyn computer software (Biosoft, Cambridge, UK) was employed to determine the combination effect of vorinostat/topotecan and cisplatin by graphing the combination index (CI) on fraction affect-CI plots. A CI value greater than 1 signifies an antagonistic interaction, whereas a CI value of 1 signifies an additive interaction and a CI value less than 1 signifies a synergistic interaction.

Chapter 3: Results

3.1 ATF3 is a target of platin cytotoxicity in NSCLC

The cytotoxic effects of platins, specifically cisplatin and carboplatin, were previously evaluated in various human cancer cell lines [101]. The induction of ATF3 by both platins was observed at the protein and mRNA levels [101]. In order to further confirm ATF3's role in platin cytotoxicity, ATF3-/- and wild type (ATF3+/+) MEFs were employed. Both cell lines were treated with cisplatin (0-6μg/mL), carboplatin (0-200μg/mL) as well as with docetaxel (0-50nM), that targets tubulin cytoskeleton architecture [153], for 48 hours. MTT cell viability assay was used to determine that the ATF3-/- MEFs display less sensitivity to both platins compared to the wild type MEFs (Figure 3.1, A and B). However, there was no difference in sensitivity between the wild type and ATF3-/- MEFs after treatment with docetaxel (Figure 3.1C). Overall, this demonstrates a role for ATF3 in regulating platin cytotoxicity.

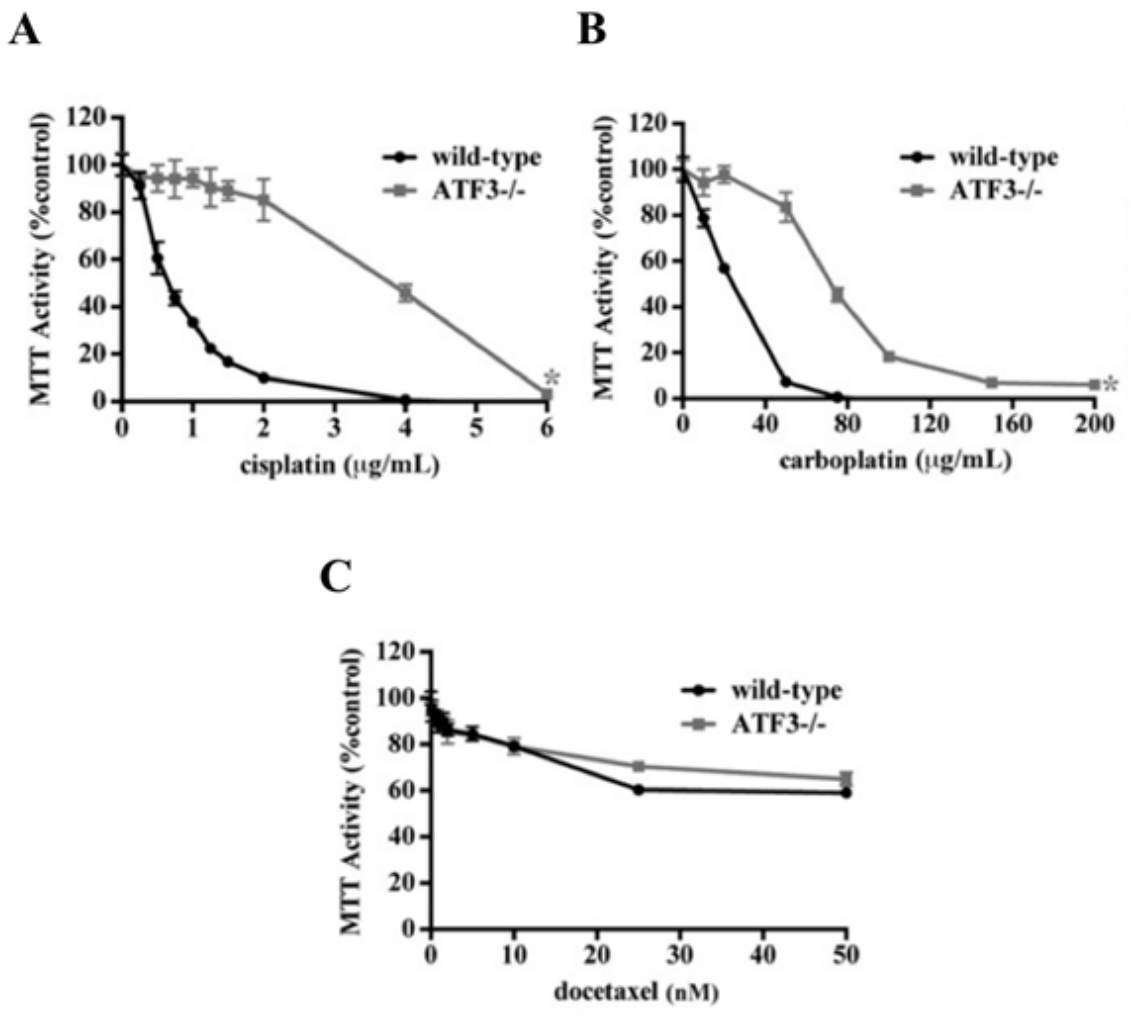

Figure 3.1. Platin cytotoxicity evaluated in wild type and ATF3-/- MEFs by MTT cell viability assay. Wild type and ATF3-/- MEFS were treated with **A)** 0-6μg/mL cisplatin, **B)** 0-200μg/mL carboplatin and **C)** 0-50nM docetaxel (C), and assessed by MTT cell viability assay following treatment for 48 hours. Cell viability was determined against untreated cells, which were assigned to represent 100%. Platin cytotoxicity was confirmed to be ATF3 dependent, while docetaxel was not. Significant difference in the viability curves comparing the wild type and ATF3-/- MEFs responses represented by * = $p<0.05$.

Resistance to platins is widely recognized as a limiting factor for their utilization in the clinical setting for NSCLC [80]. Therefore, in order to further identify potential mediators of resistance in NSCLC, several cisplatin-resistant clones were established from two NSCLC cell lines, Calu6 and H23 [104]. As previously mentioned, both parental cell lines are adenocarcinoma with genetic mutations in p53 and KRAS [142,143]. Once established through cisplatin exposure, the sensitivity of these cisplatin-resistant sub-lines, referred to as Calu6cisR1-3 and H23cisR1-3, to cisplatin and carboplatin compared to the parental cell lines, was confirmed. Both the parental and the cisplatin-resistant cell lines were treated with a range of cisplatin and carboplatin concentrations for 48 hours. MTT cell viability assays, demonstrated that the Calu6cisR1-3 and H23cisR1-3 sub-lines displayed less sensitivity to the platins in comparison to their respective parental cell lines [104]. In this study, Calu6 and H23, and one representative cisplatin-resistant sub-line, Calu6cisR1 and H23cisR1, were employed. I confirmed this differential sensitivity between the Calu6, H23 and their respective cisR1 sub-lines following treatment with cisplatin (0-4 μg/mL) for 48 and 72 hours by MTT assays. (Figure 3.2, A-D)

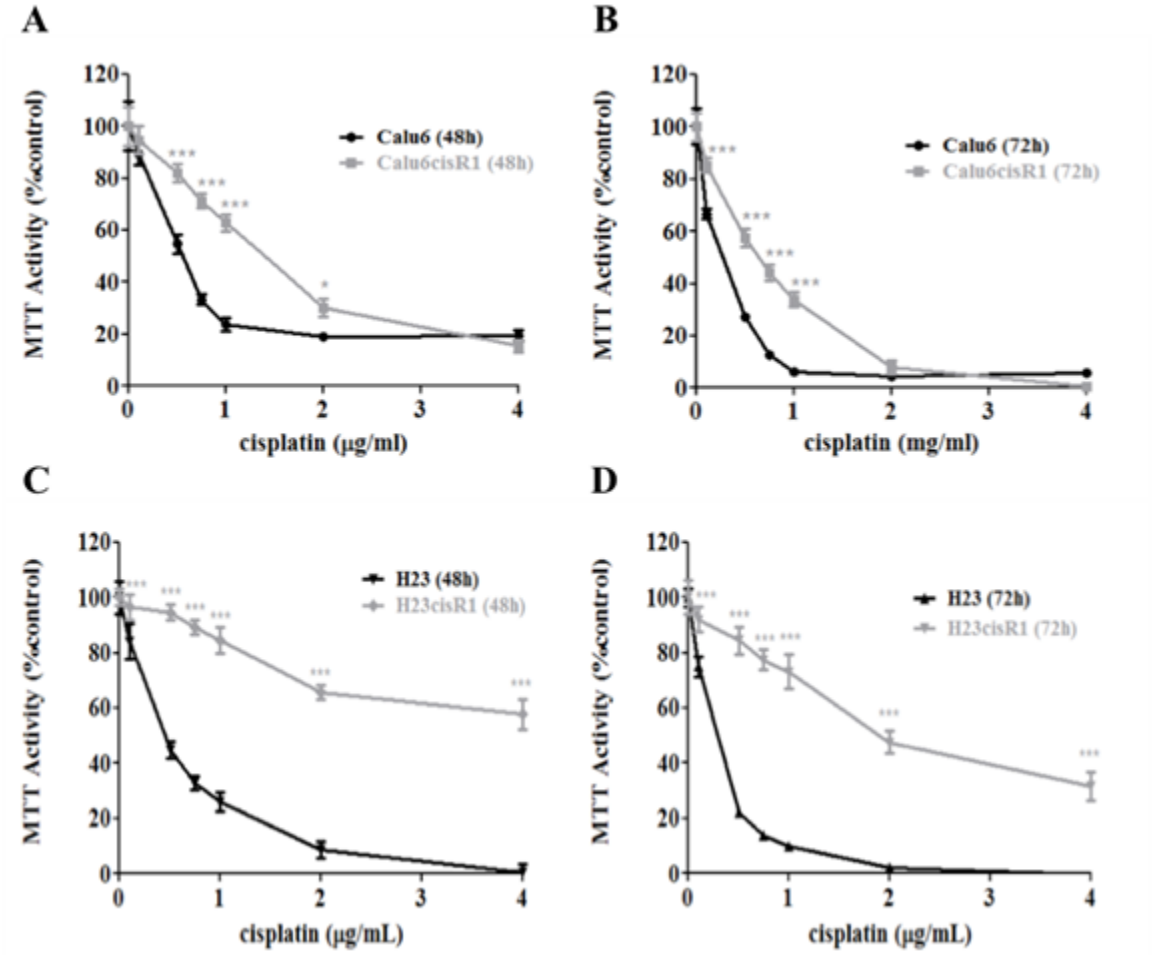

Figure 3.2. Platin cytotoxicity evaluated in NSCLC cell lines Calu6, H23 and their cisplatin resistant sub-lines, Calu6cisR1 and H23cisR1, respectively, by MTT cell viability assay. All four cell lines were treated with 0-4µg/mL cisplatin assessed by MTT assay following treatment for 48 **(A,C)** and 72 **(B,D)** hours. Cell viability was determined against untreated cells, which were assigned to represent 100%. Differential sensitivity to cisplatin was confirmed in between both parental and cisplatin-resistant cell lines after 48 and 72 hours. Error bars represent SD from the mean of n=3 experiments. Significant difference in the viability curves comparing parental and cisplatin-resistant responses to cisplatin represented by * = $p<0.05$, ** = $p<0.01$ and *** = $p<0.001$.

Using RNA-Seq Transcriptome Analysis, we identified genes that were differentially expressed between the parental cell lines and their resistant sub-line following cisplatin treatment. ATF3 was the most significant differentially induced gene between the parental and their respective cisR1 sub-lines following treatment with cisplatin (2μg/mL) for 24 hours (Figure 1.4A and B). This differential expression was also observed at both the mRNA and protein levels (Figure 1.4C and D). In this study, these parental cell lines and their respective cisplatin-resistant sub-lines were treated with various drugs that have previously been identified as ATF3 inducers such as doxorubicin (5μM), thapsigargin (1μM), vorinostat (10μM), lovastatin (10μM) and GGTI-298 (10μM) in addition to cisplatin (1μg/mL). Following 24 hours of treatment, Western blot analysis was performed to compare ATF3 expression between parental and cisplatin-resistant cell lines (Figure 3.3). A 24 hour time point was chosen to evaluate ATF3 expression as previous reports have shown its upregulation at that time following cisplatin treatment [101,154]. Additionally, it was the time point used for the RNA-seq analysis, where differential ATF3 expression was observed between the parental and cisR1 cell lines. Cisplatin and doxorubicin treatments induced ATF3 expression in the parental cell lines only. Thapsigargin and vorinostat induced ATF3 expression in both parental and cisplatin resistant cell lines. Thapsigargin and vorinostat are known inducers of ATF3 through the ISR pathway [122,126]. ATF3 induction was not observed in the Calu6 and Calu6cisR1 following treatment with lovastatin and GGTI-298, which target the mevalonate pathway and induce metabolic stress [125,155]. A weak induction of ATF3 was observed in both H23 and H23cisR1 following treatment with lovastatin. Overall, these preliminary results obtained showed that the DNA damaging agents tested displayed differential induction of

ATF3 in the parental and resistant sub-lines but not the ISR and metabolic stress agents tested.

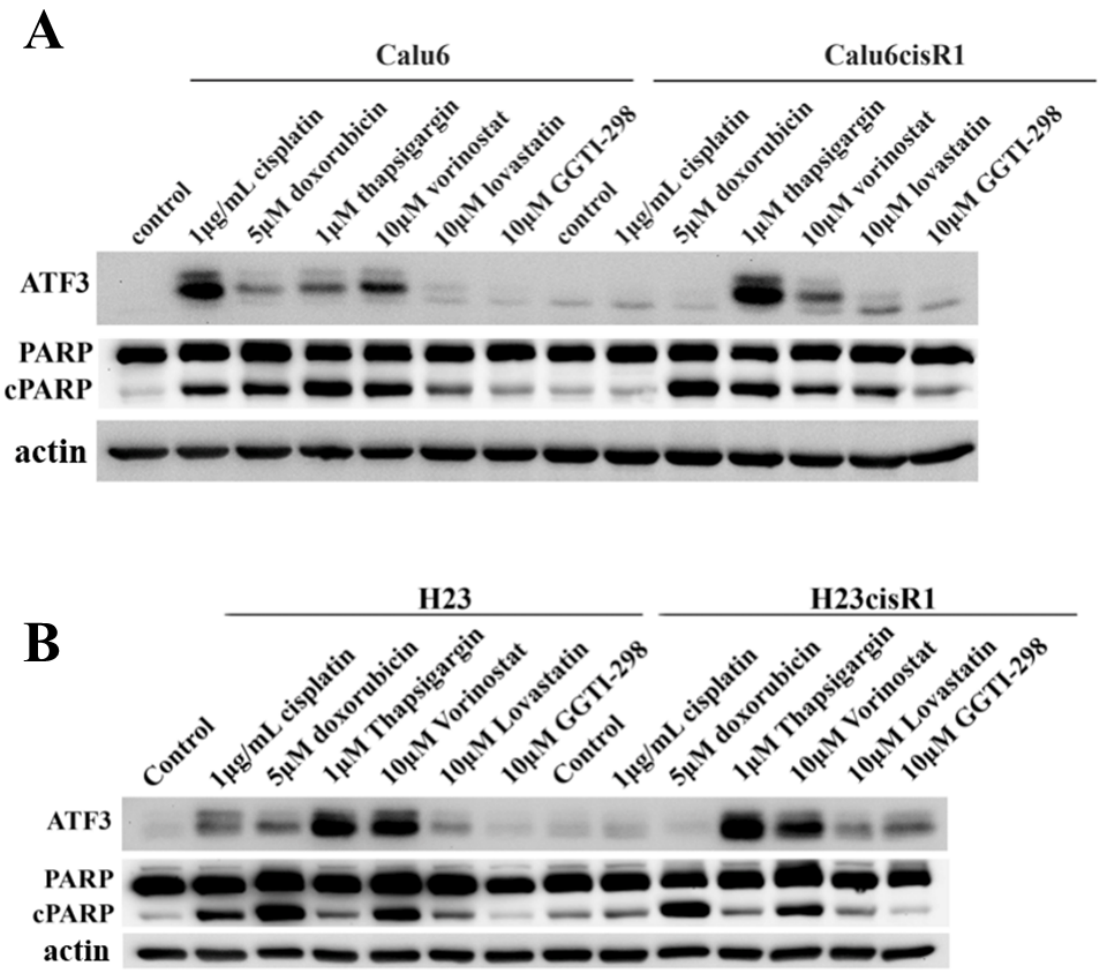

Figure 3.3. Evaluation of ATF3 expression between the parental cell lines Calu6 and H23 and their cisplatin-resistant sub-lines, Calu6cisR1 and H23cisR1, after treatment with various ATF3 inducers. All four cell lines were treated with 1μg/mL cisplatin, 5μM doxorubicin, 1μM thapsigargin, 10μM vorinostat, 10μM lovastation and 10μM GGTI-298 for 24 hours. Following the treatment, western blot analysis was performed in order to evaluate the ATF3 expression and PARP cleavage. Actin was used as a loading control.

3.2 Various pathways, including the DDR, ISR and MAPK signalling, play a role in cisplatin induced ATF3 expression

A number of stress signalling pathways play a role in the induction of ATF3 [120]. These include the ISR mediated by ATF4 induced by reactive oxygen species (ROS) [128], components of the MAPK pathway [127] and the DNA-damage response, including ATM and p53 proteins [111,115]. To delineate the pathways regulating cisplatin induced ATF3 expression, specific inhibitors of these pathways were employed.

Cisplatin has been previously shown to induce ROS formation following oxidative stress leading to cell death [84]. Therefore, to evaluate the role of cisplatin-induced ROS in the induction of ATF3 in NSCLC cells, Calu6 and H23 cell lines were pre-treated for one hour with 10mM N-acetylcysteine (NAC), a ROS scavenger, followed by treatment with cisplatin (0,1,2,4,8μg/mL) for 24 hours (Figure 3.4, A and B). Western blot analysis was performed to evaluate ATF3 expression and PARP cleavage, a marker of apoptosis [156]. In both cell lines, the induction of ATF3 was attenuated, particularly at 4μg/mL in Calu6 and 2μg/mL in H23, which were the concentrations that induced the highest ATF3 expression following cisplatin treatment alone in the respective cell lines. Furthermore, higher levels of cleaved PARP (cPARP), were observed with cisplatin treatments alone in both parental cell lines, compared to the co-treatments with NAC, specifically at 2 and 4μg/mL in the Calu6 cell line and 8μg/mL in the H23 cell line, suggesting a role for ROS in cisplatin-induced ATF3 expression and apoptosis. The lack of ATF3 induction with 8μg/mL cisplatin can be attributed to increased cell death.

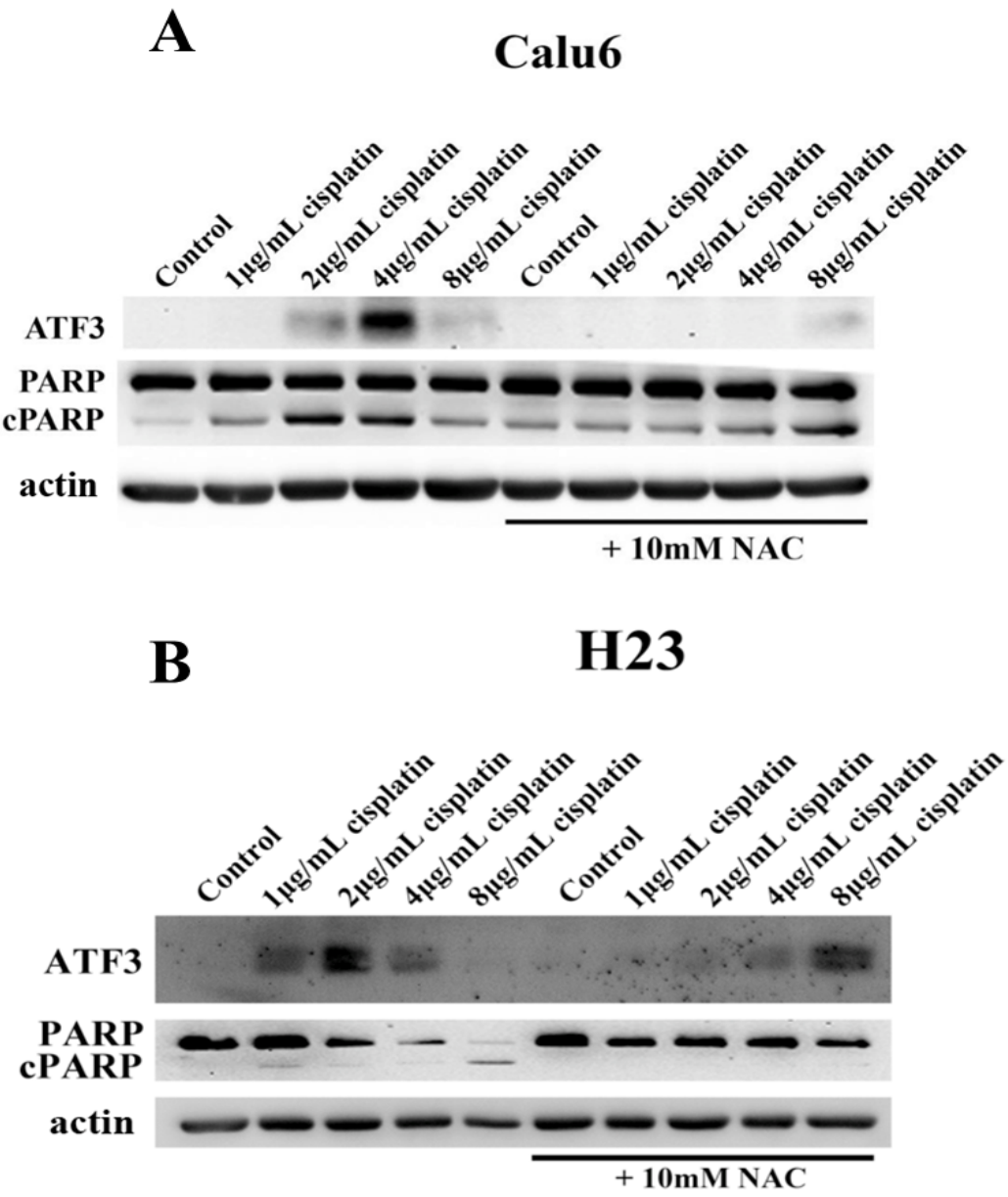

Figure 3.4. The role of ROS in cisplatin cytotoxicity in Calu6 and H23 cell lines. Calu6 **(A)** and H23 **(B)** were treated with 10mM NAC alone for 1 hour prior to co-treatment with cisplatin for 24 hours. Western blot analysis was performed to evaluate ATF3 expression and PARP cleavage. Cisplatin-induced ATF3 expression was attenuated with NAC treatment in both cell lines. Actin was used as a loading control.

The role of the DDR in cisplatin-induced ATF3 expression in NSCLC cells was evaluated by using KU55933, an ATM inhibitor that induces G1 cell cycle arrest allowing for repair of DNA damage [157]. As previously mentioned, ATM is a key kinase in the DDR pathway that can lead to apoptosis [96]. Calu6 and H23 were pre-treated with 10μM KU55933 for 1 hour prior to co-treatment with cisplatin (0,1,2,4,8μg/mL) for 24 hours. There was no pronounced difference between the ATF3 expression in both cell lines in the presence and absence of KU55933 following Western blot analysis (Figure 4.5, A and B), while a modest decrease in cPARP was observed with 10μM KU55933 in the H23 cell line (Figure 3.5B).

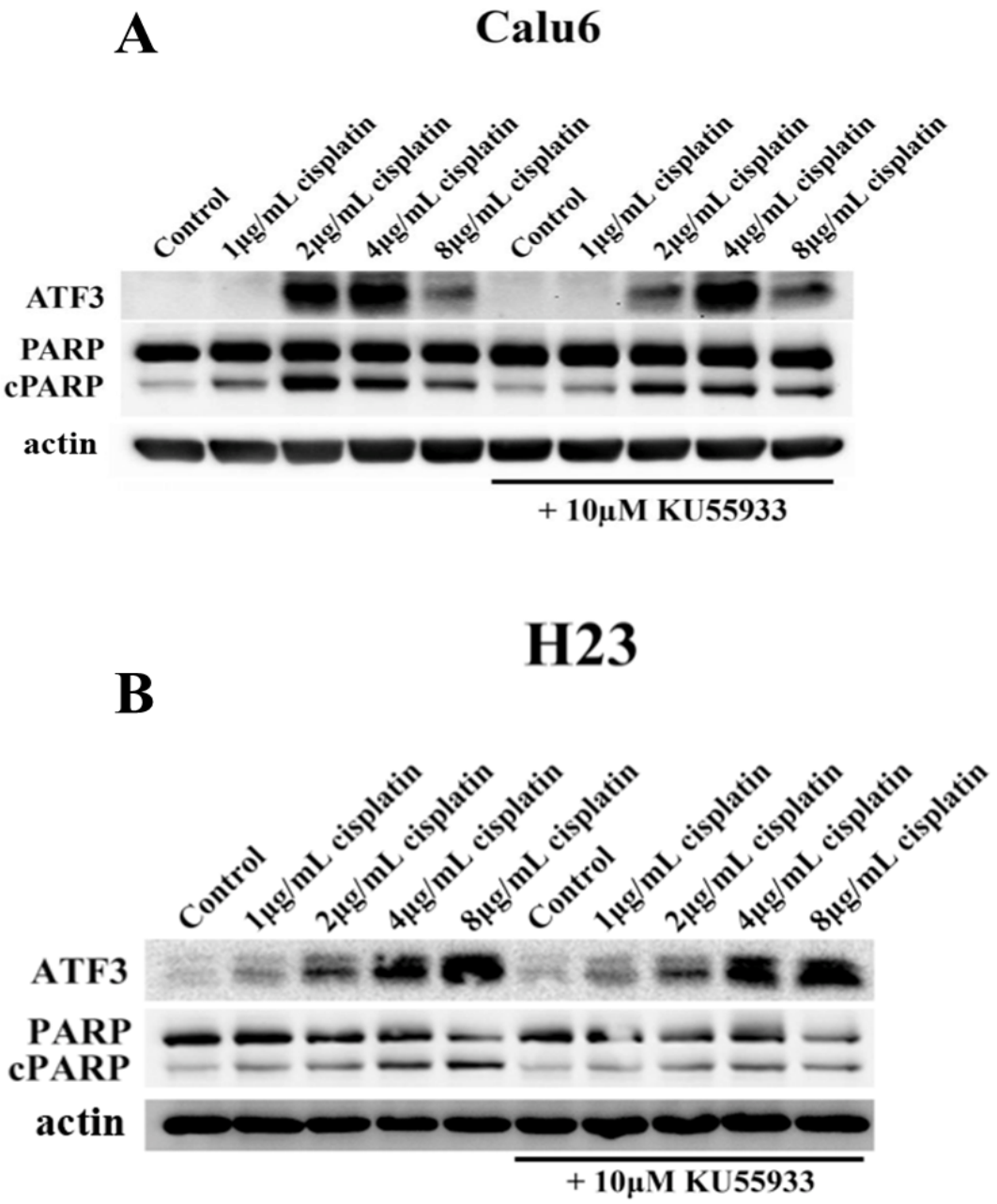

Figure 3.5. The role of the DDR pathway in cisplatin cytotoxicity in Calu6 and H23 cell lines. Calu6 **(A)** and H23 **(B)** were treated with 10μM KU55933 (ATM inhibitor) for 1 hour prior to co-treatment with cisplatin for 24 hours. Western blot analysis was performed to evaluate ATF3 expression and PARP cleavage. No pronounced difference was observed with KU55933 in both cell lines. Actin was used as a loading control.

The MAPK signalling pathway has been identified to play a role in cisplatin cytotoxicity as well as ATF3 expression [83,101,127]. Moreover, our laboratory previously linked these two events by identifying ATF3 as a key target of cisplatin cytotoxicity through the MAPK signalling pathway [101]. Work done previously in our laboratory showed that the JNK pathway played a role in cisplatin-induced ATF3 expression [104]. To evaluate this further, Calu6 and H23 cell lines were pre-treated with 25μM SP600125, a JNK inhibitor, followed by co-treatment with cisplatin (0,1,2,4,8μg/mL) for 24 hours. Western blot analysis performed following this treatment displayed attenuated ATF3 expression in the H23 cell line (Figure 3.6B), while it was not as pronounced in the Calu6 cell line (Figure 3.6A). No pronounced differences were seen in the expression levels of PARP cleavage with and without the JNK inhibitor. The differential phosphorylation levels of c-Jun were assessed as a control for SP600125 activity. As a member of the AP-1 family, c-Jun can be induced in response to genotoxic stress, which includes DNA damaging agents such as cisplatin [158,159]. Furthermore, upon its activation by phosphorylation, the ubiquitination of c-Jun is reduced which leads to its stabilization [160]. This provides a potential explanation regarding the increasing levels of total c-Jun that is observed in Figure 3.6.

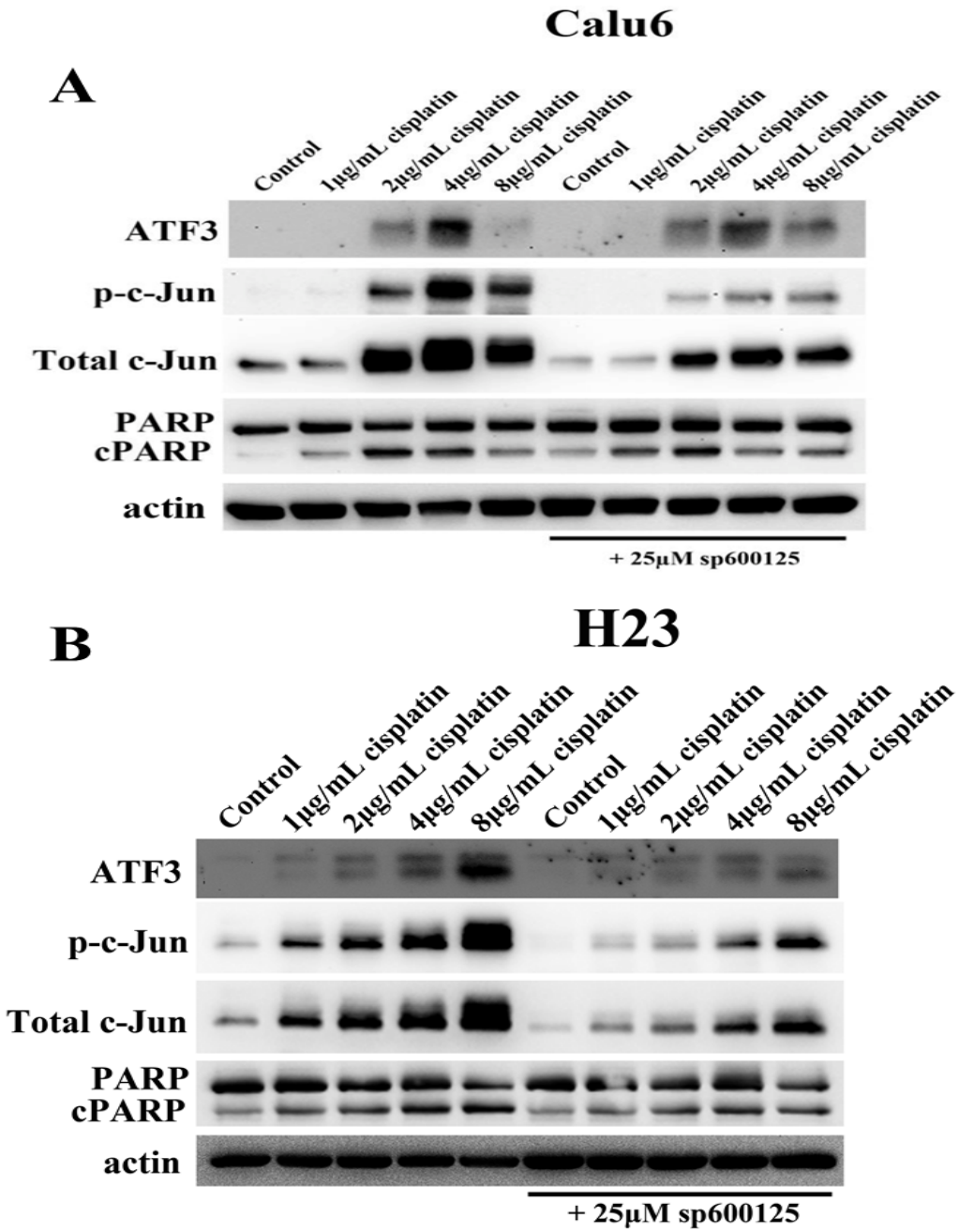

Figure 3.6. The role of the MAPK pathway in cisplatin cytotoxicity in Calu6 and H23 cell lines. Calu6 **(A)** and H23 **(B)** were treated with 25µM SP600125 (JNK inhibitor) for 1 hour prior to co-treatment with cisplatin for 24 hours. Western blot analysis was performed to evaluate ATF3 expression and PARP cleavage. Cisplatin-induced ATF3 expression was attenuated following SP600125 treatment in both cell lines. Phosphorylation of c-Jun was used as a control for SP600125 efficacy and actin was used as a loading control.

3.3 ATF3 inducers, vorinostat and topotecan, enhance cisplatin cytotoxicity

ATF3 can be induced by a variety of different pathways and its sustained induction can drive apoptosis [119,120]. Thus combining ATF3 inducers with cisplatin has the potential to be an effective therapeutic approach through enhancing and sustaining ATF3 expression. In order to identify such novel ATF3 inducers, our laboratory employed a chemical library of 1200 FDA approved compounds, obtained from Prestwick Laboratories, to identify compounds that enhance cisplatin cytotoxicity in Calu6 cells. Calu6 cells was pre-treated with 1μM of the library agents for 24 hours, followed by a 0.4μg/mL cisplatin for 48 hours, for a total treatment duration of 72 hours. The cytotoxicity of the combination was evaluated by MTT assays and compounds that displayed an enhanced cisplatin cytotoxicity of at least 20% were identified as hits (Table 1a). Secondly, it was of interest to identify compounds whose cytotoxicity is also dependent on ATF3. In this screen, wild type and ATF3-/- MEFS were treated with 5μM of the library agents for 48 hours and evaluated employing MTT assays. Compounds whose cytotoxicity between the wild type and ATF3-/- MEFS differed by at least 20% were identified as hits (Table 1b). Two compounds that were identified as hits in both screens were the HDACi vorinostat, and topoisomerase I inhibitor topotecan. Interestingly, our lab previously identified another HDACi, M344, as an ATF3 inducer that enhances cisplatin cytotoxicity [126]. Vorinostat and topotecan were further evaluated as potential ATF3 inducers and in combination with cisplatin as potential enhancers of this important chemotherapeutic drug.

MTT cell viability assays were performed in wild type and ATF3-/- MEFs in order to evaluate their sensitivity to vorinostat (0-10μM) and topotecan (0-10μM) after 48

hours to validate the screen data. Differential sensitivity was observed between the two cell lines with both vorinostat and topotecan (Figure 3.7, A and B) as a decrease in sensitivity was observed in the ATF3-/- MEFs compared to their wild type counterpart, thus suggesting a role for ATF3 in vorinostat and topotecan induced cytotoxicity. Calu6, H23 and their cisplatin-resistant sub-lines were treated with vorinostat (0-10μM) and topotecan (0-4μM) for 48 hours and evaluated using MTT assays, in order to assess whether these NSCLC parental and cisplatin-resistant cell lines display differential sensitivity to these compounds. Both cisR1 sub-lines displayed less sensitivity to vorinostat compared to their respective parental cell lines (Figure 3.7, C and D). Differential sensitivity to topotecan was observed between the parental and cisR1 sub-lines but the difference in cell viability was modest (Figure 3.7, E and F).

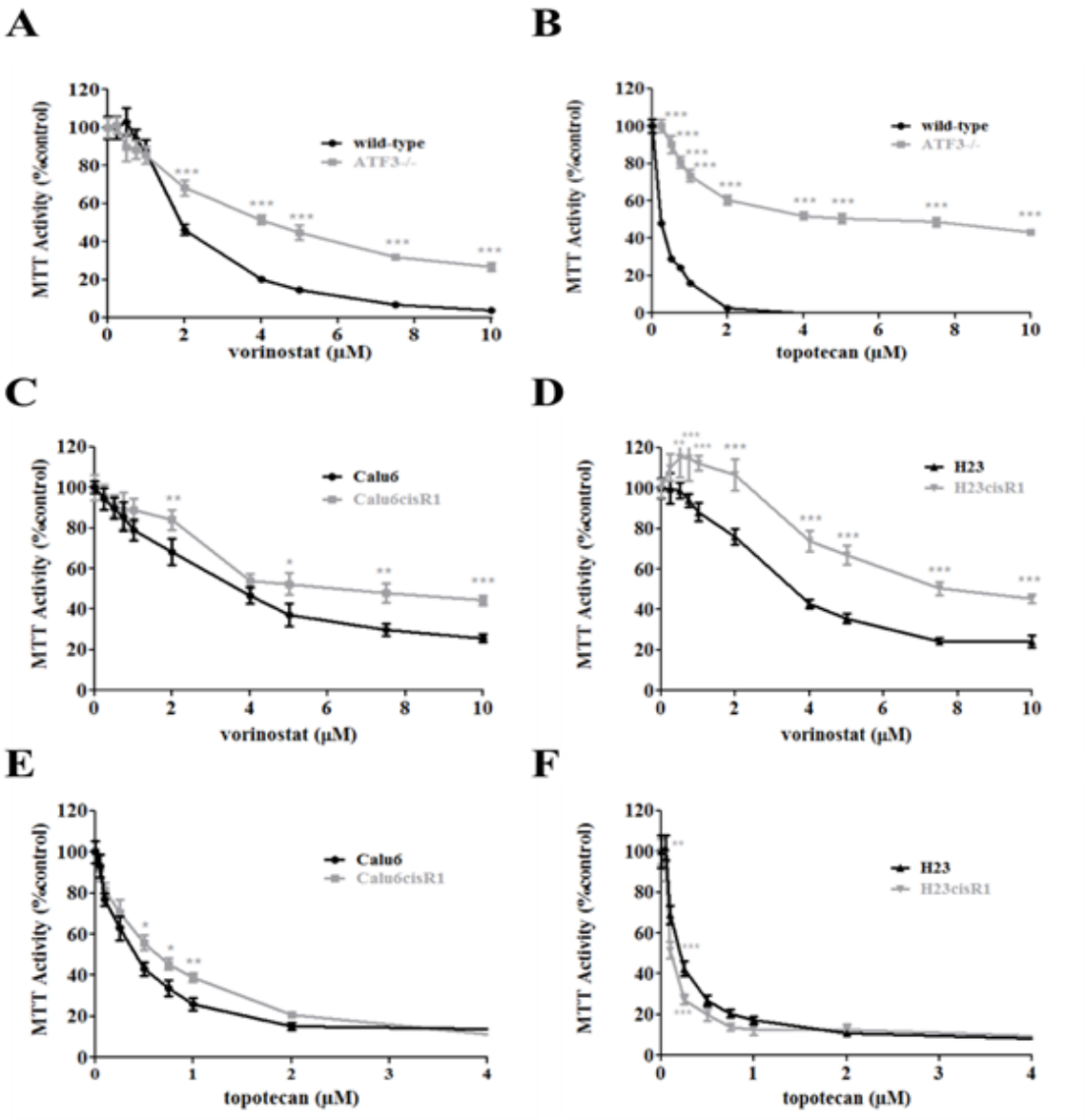

Figure 3.7. Vorinostat and topotecan cytotoxicity evaluated in wild type and ATF3-/- MEFs and NSCLC cell lines by MTT cell viability assay. The sensitivity of wild type and ATF3-/- MEFs to 0-10μM vorinostat **(A)** and 0-10μM topotecan **(B)** was assessed by MTT cell viability assay following treatment for 48 hours. The ATF3-/- MEFS displayed less sensitivity to vorinostat and topotecan compared to their wild type counterparts. Sensitivity to vorinostat (0-10μM) and topotecan (0-4μM) was assessed in Calu6 and Calu6cisR1 **(C and E)** as well as H23 and H23cisR1 **(D and F)** by MTT cell viability assay following treatment for 48 hours. Cell viability was determined against untreated cells, which were assigned to represent 100%. Differential sensitivity to vorinostat was observed between the parental and cisplatin-resistant cell lines. Differential sensitivity to topotecan was observed between the parental and cisR1 sub-lines as well but the difference in cell viability was modest. Error bars represent SD from the mean of n=3 experiments. Significant differences represented by * = $p<0.05$, ** = $p<0.01$ and *** = $p<0.001$.

Furthermore, Western blot analysis displayed a dose-dependent increase in ATF3 expression and PARP cleavage in Calu6 and H23 as well as their cisplatin-resistant counterparts, Calu6cisR1 and H23cisR1 following treatment with vorinostat (0,1,2,5,7.5,10μM) for 24 hours (Figure 3.8A). The levels of ATF3 expression and PARP cleavage induced following vorinostat treatment were reduced in the cisplatin-resistant cell lines compared to the parental cell lines. Western blot analysis also showed a dose dependent induction of ATF3 in Calu6, H23 and their respective cisplatin-resistant sub-lines following treatment with topotecan (0,1,2,5,7.5,10μM for Calu6 and Calu6cisR1, 0,0.01,0.05,0.1,0.5,1μM for H23 and H23cisR1) (Figure 3.8B). However, lower concentrations of topotecan were used for the H23 and H23cisR1 cell lines due to a difference in sensitivity compared to Calu6 and Calu6cisR1. The levels of ATF3 expression and PARP cleavage were relatively lower in H23cisR1 compared to H23 following treatment with topotecan, while no difference was seen between the Calu6 and Calu6cisR1.

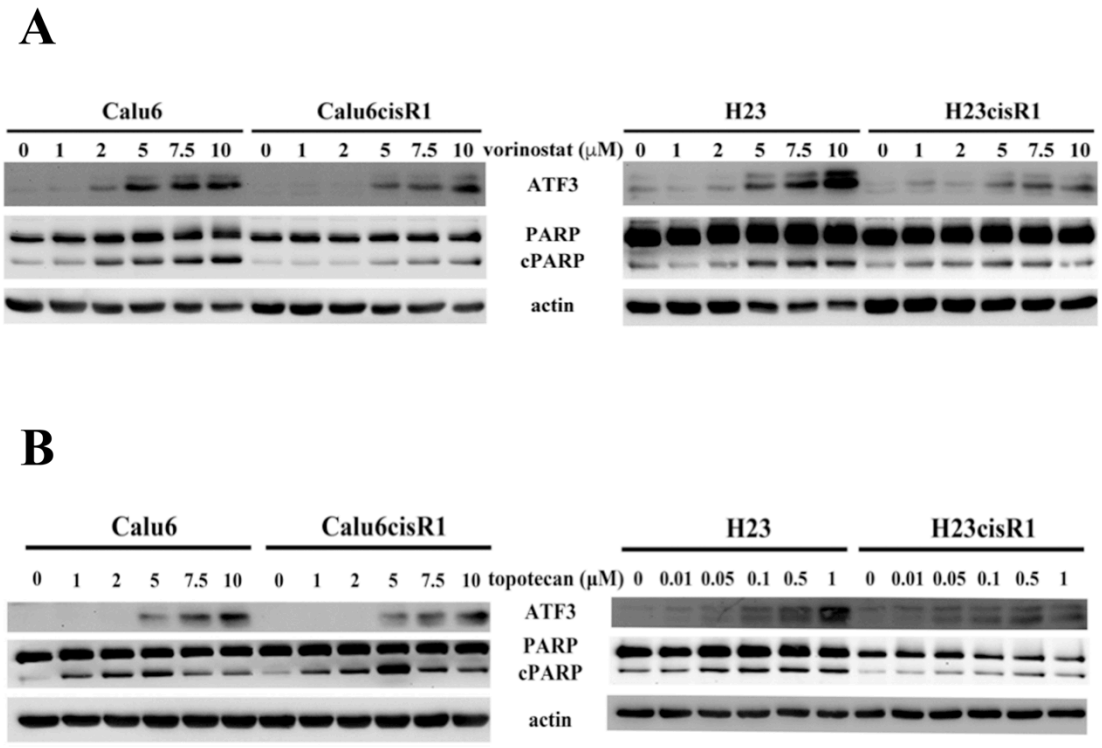

Figure 3.8. Induction of ATF3 expression by vorinostat and topotecan in Calu6, H23 and their cisR1 sub-lines. All four cell lines were treated vorinostat (0-10μM) **(A)** and topotecan (0-10μM for Calu6 and Calu6cisR1, 0-1μM for H23 and H23cisR1) **(B)** for 24 hours. Western blot analysis was performed to evaluate ATF3 expression and PARP cleavage. A dose-dependent induction of ATF3 expression was observed in all four cell lines. Actin was used as a loading control.

Next, combinations of cisplatin and vorinostat were evaluated in the parental Calu6 and H23 cell lines along with cisplatin-resistant sub-lines. These treatments consisted of 24 hour pre-treatments with vorinostat (1,2,5μM) followed by a combination of cisplatin (0-4μg/mL) and vorinostat for 48 hours, for a total duration of 72 hours treatments, which represents the same sequence of drug treatment that was previously performed in the library screen. MTT cell viability assays showed enhanced cytotoxicity with the combination compared to cisplatin treatment alone in all four cell lines tested (Figure 3.9). A combination index (CI) analysis determined that the combination of cisplatin and vorinostat resulted in a synergistic effect, especially with 2μM vorinostat, in both parental and cisplatin-resistant cell lines (Figure 3.10). The analysis was performed using the Calcusyn software, which is based on the method described by T-C Chou [161]. A CI value greater than 1 signifies an antagonistic interaction, a CI value of 1 signifies an additive interaction and CI values less than 1 signifies a synergistic interaction.

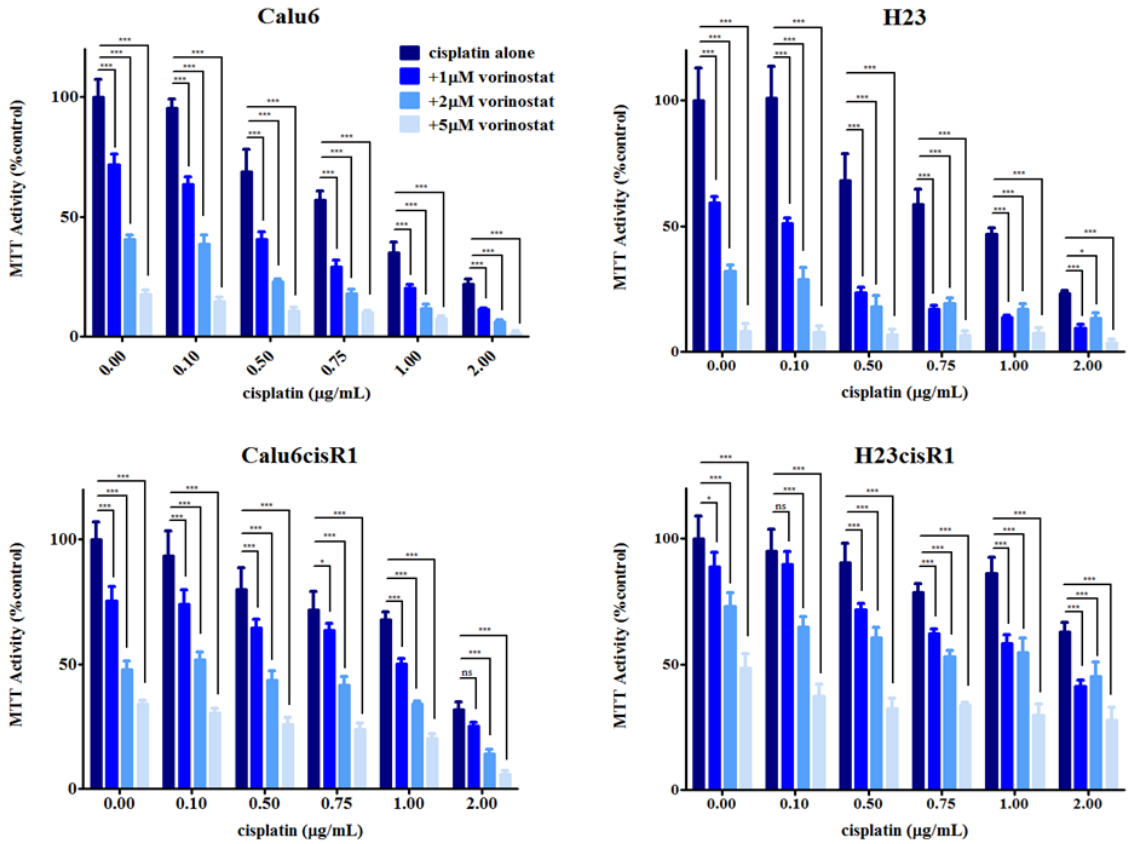

Figure 3.9. Combination of cisplatin and vorinostat cytotoxicity evaluated in Calu6, H23 and their cisR1 sub-lines by MTT cell viability assay All four cell lines were treated with a combination of 1,2 or 5μM vorinostat and 0-4μg/mL cisplatin for 72 hours (24 hours vorinostat pre-treatment + 48 hours cisplatin and vorinostat combination). Cell viability was determined against untreated cells, which were assigned to represent 100%. Enhanced cytotoxicity was observed with the combinations compared to cisplatin treatment alone. Error bars represent SD from the mean of n=3 experiments. Significant differences represented by * = $p<0.05$, ** = $p<0.01$ and *** = $p<0.001$, while ns = not significant.

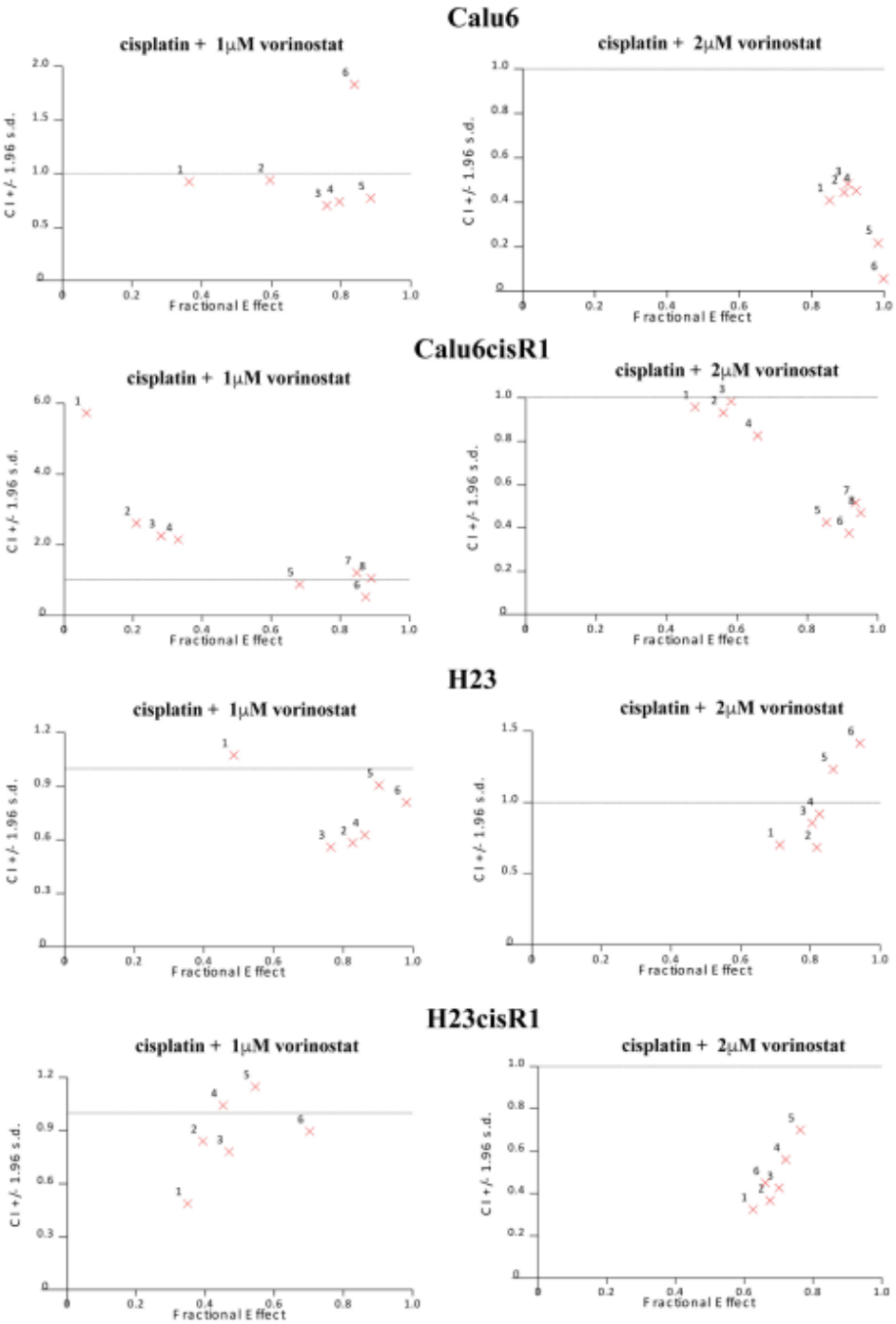

Figure 3.10. Fa-CI plots for cisplatin and vorinostat combination in Calu6, H23 and their cisplatin-resistant sub-lines. Combination index analysis of cisplatin and vorinostat (1 and 2μM) based on MTT cell viability assays (24 hours vorinostat pre-treatment + 48 hours of cisplatin and vorinostat combination). Vorinostat and cisplatin displayed a synergistic effect. The Fa-CI plots were generated using the CalcuSyn software. A CI value greater than 1 signifies an antagonistic interaction, whereas a CI value of 1 signifies an additive interaction and a CI value less than 1 signifies a synergistic interaction.

Similarly, MTT assays were performed to evaluate the combination of cisplatin and topotecan in these NSCLC cell lines. The parental cell lines, Calu6 and H23, and their respective cisR1 sub-lines, Calu6cisR1 and H23cisR1, were treated with topotecan (0.01,0.02 and 0.04μM) for 24 hours, followed by a combination of cisplatin (0-4μg/mL) and topotecan for 48 hours, for a total treatment time of 72 hours. MTT assays were used to evaluate the cytotoxicity of the combination. The combination of cisplatin displayed enhanced cytotoxicity compared to cisplatin alone (Figure 3.11). Combination index analysis of this treatment further displayed a synergistic effect at several cisplatin doses in these cell lines (Figure 3.12).

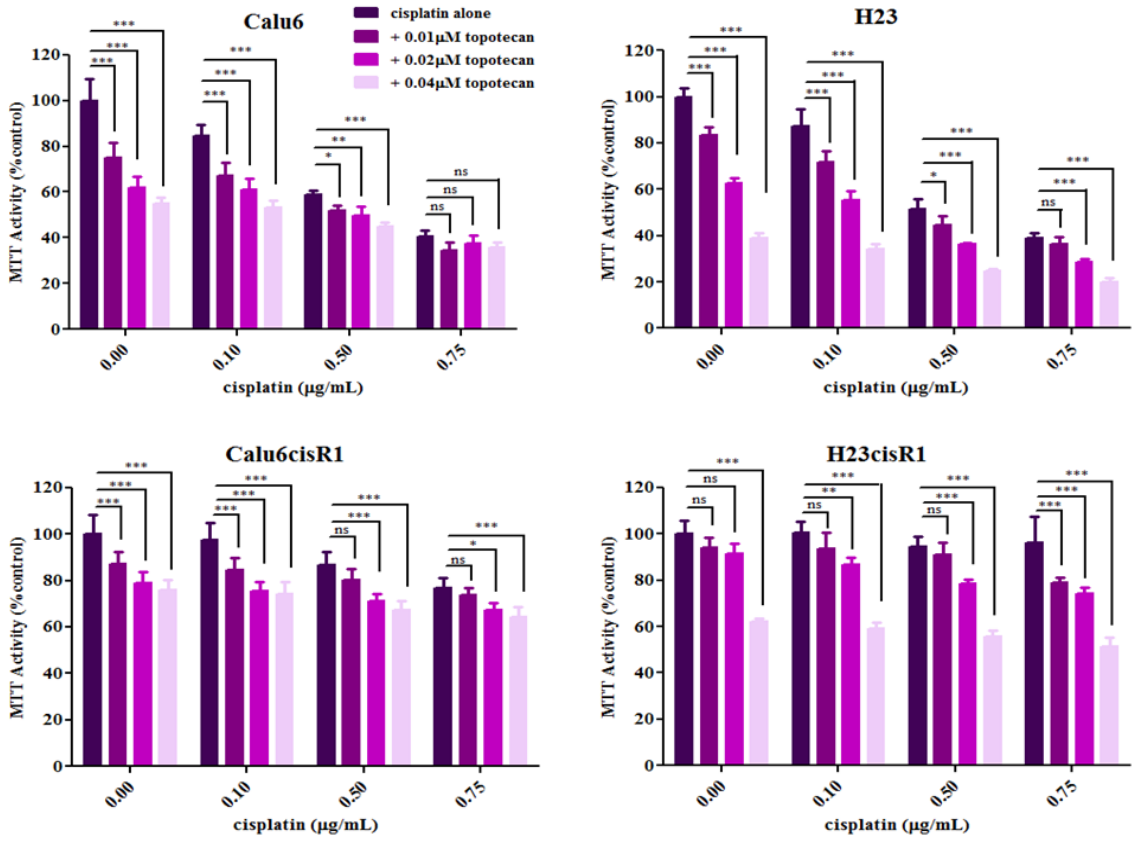

Figure 3.11. Combination of cisplatin and topotecan cytotoxicity evaluated in Calu6, H23 and their cisR1 sub-lines by MTT cell viability assay. All four cell lines were treated with a combination of 0.01,0.02 or 0.04μM topotecan and 0-4μg/mL cisplatin for 72 hours (24 hours topotecan pre-treatment + 48 hours cisplatin and topotecan combination). Cell viability was determined against untreated cells, which were assigned to represent 100%. Enhanced cytotoxicity was observed with the combinations compared to cisplatin treatment alone. Error bars represent SD from the mean of n=3 experiments. Significant differences represented by * =$p<0.05$, ** = $p<0.01$ and *** = $p<0.001$, while ns = not significant.

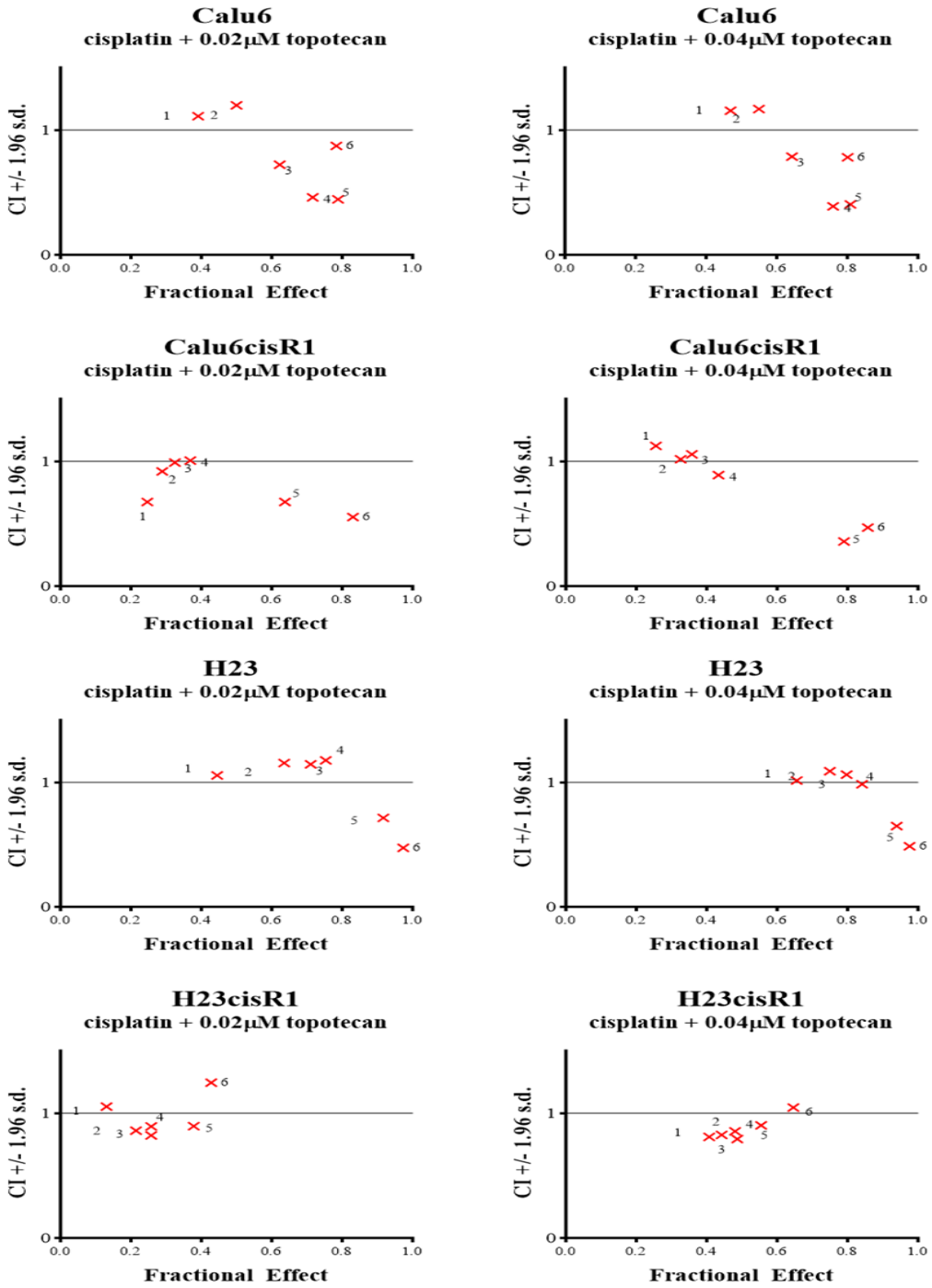

Figure 3.12. Fa-CI plots for cisplatin and topotecan combination in Calu6, H23 and their cisplatin-resistant sub-lines. Combination index analysis of cisplatin and topotecan (0.02 and 0.04μM) based on MTT cell viability assays (24 hours topotecan pre-treatment + 48 hours of cisplatin and topotecan combination). Topotecan and cisplatin displayed a synergistic effect at certain doses. The Fa-CI plots were generated using the CalcuSyn software. A CI value greater than 1 signifies an antagonistic interaction, whereas a CI value of 1 signifies an additive interaction and a CI value less than 1 signifies a synergistic interaction.

Following assessing the cytotoxicity of the combinations, Western blot analysis was performed to evaluate the ATF3 expression following pre-treatment with 5μM vorinostat for 24 hours, followed by the addition of cisplatin (2,4 μg/mL) for another 24 hours, for a total of 48 hours. The rationale behind the time points used was to recapitulate the 24 hours pre-treatment with vorinostat performed in the library screen, followed by the combination of vorinostat and topotecan. However, the combination was evaluated for 24 hours instead of 48 hours in the Western blot analyses due to the increased cell death preventing the assessment of ATF3 expression levels. Following the treatments, Western blot analysis displayed an increase in ATF3 expression with the combination of cisplatin and vorinostat in both cisplatin-resistant cells compared to cisplatin and vorinostat treatments alone, thus suggesting that this combination is rescuing the aberrant ATF3 induction in these cells (Figure 3.13A). Similarly, the cisplatin-resistant cell lines were pre-treated with topotecan (0.5μM for Calu6cisR1, 0.1μM for H23cisR1), followed the addition of cisplatin (2 and 4μg/mL for Calu6cisR1, 1 and 2μg/mL for H23cisR1) for another 24 hours, for a total of 48 hours of treatment. Western blot analysis was performed and the combination of cisplatin and topotecan also displayed an enhanced ATF3 expression compared to cisplatin and topotecan alone in the Calu6cisR1 sub-line (Figure 3.13B). In the H23cisR1 sub-line, enhanced ATF3 expression was observed with 1μg/mL cisplatin in combination with 0.1μM topotecan, compared to each of those concentrations alone (Figure 3.13B). This also suggests that the combination of cisplatin and topotecan is rescuing the aberrant ATF3 induction in the cisplatin-resistant cell lines.

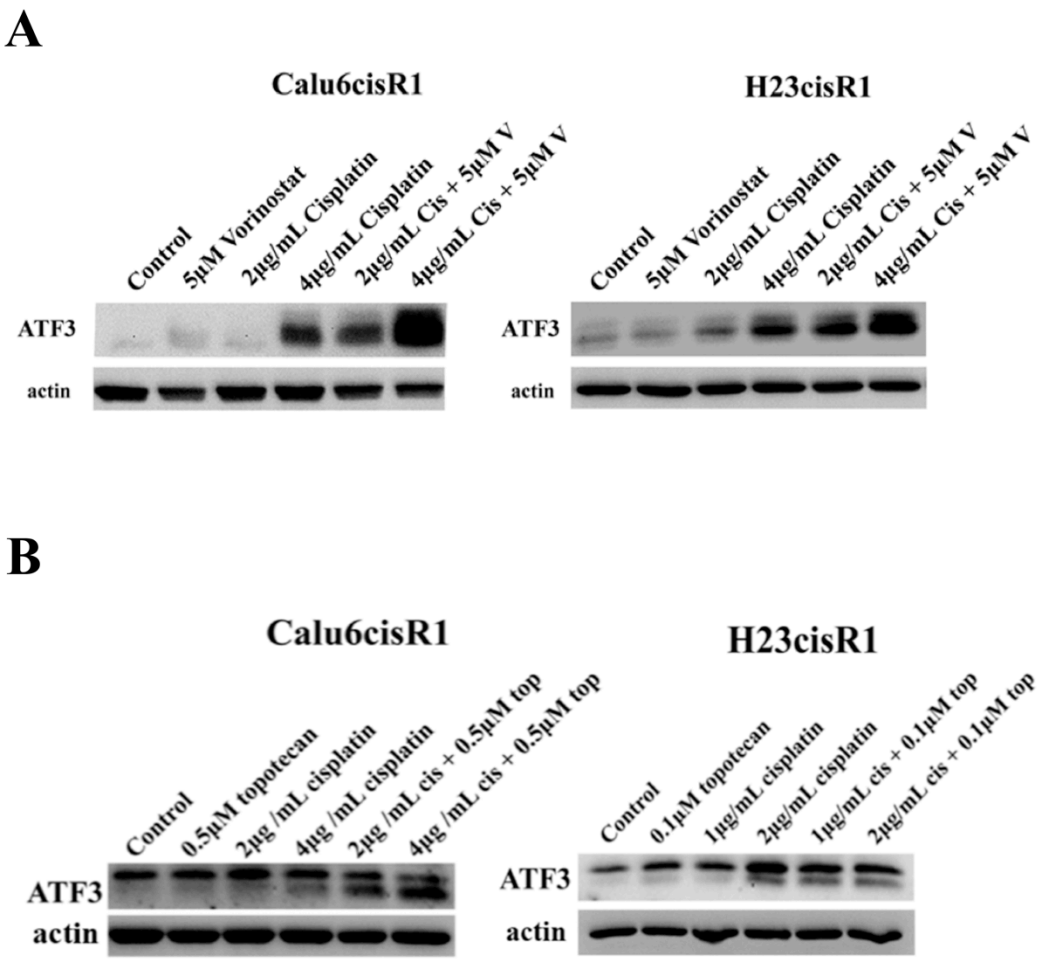

Figure 3.13. Induction of ATF3 expression by cisplatin in combination with vorinostat and topotecan in the cisR1 sub-lines. A) To evaluate the combination of cisplatin and vorinostat, Calu6cisR1 and H23cisR1 were treated with vorinostat (48 hours), cisplatin (24 hours) and a combination of cisplatin and vorinostat (48 hours). Western blot analysis was performed, where the combination of cisplatin and vorinostat displayed enhanced ATF3 induction compared to each treatment alone. **B)** The combination of cisplatin and topotecan was evaluated by treating Calu6cisR1 and H23cisR1 with topotecan (48 hours), cisplatin (24 hours) and a combination of cisplatin and topotecan (48 hours). Western blot analysis displayed that the combination of cisplatin and topotecan resulted in enhanced ATF3 induction compared to each treatment alone. Although doublet bands are shown, ATF3 expression is represented by the bottom band, while the top band consists of non-specific background detection. Actin was used as a loading control.

3.5 ATF3 is induced in *ex vivo* NSCLC tumors

In order to evaluate ATF3 expression following treatments in a more relevant clinical model, *ex vivo* NSCLC tumors and adjacent normal lung tissue from patients underdoing lobectomy were employed. The *ex vivo* NSCLC tumors as well as their adjacent normal tissue were first treated with cisplatin (0, 4, 8 μg/mL) for 48 hours. ATF3 expression was then evaluated using RT-qPCR, where ATF3 induction of greater than 5 fold of untreated tissues was observed in 3 out of the 6 tumors (Figure 3.18). However, no significant induction of ATF3 expression was observed in the normal tissue.

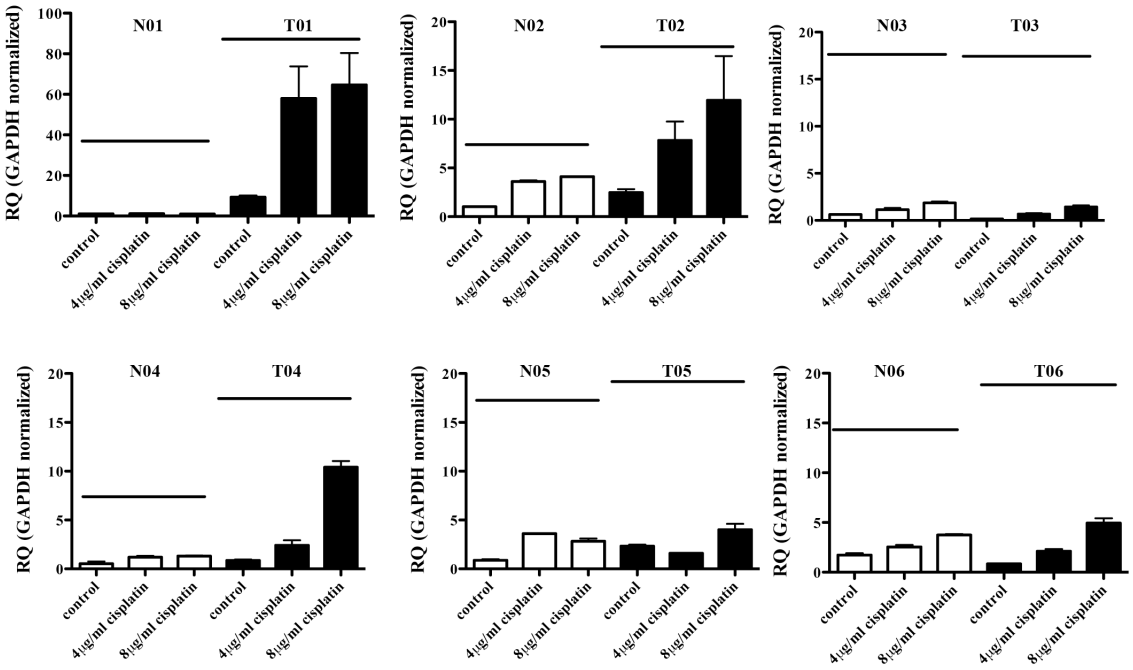

Figure 3.14. ATF3 mRNA expression levels in human NSCLC tumors and adjacent normal tissue following cisplatin treatment. Six NSCLC tumors and their adjacent normal tissue were treated with cisplatin (0,4,8 μg/mL) for 48 hours. RT-qPCR was performed to determine ATF3 mRNA expression. Three of six NSCLC tumors displayed ATF3 expression, while no induction of ATF3 was seen in the normal tissue The untreated normal tissue was used to normalize each sample and GAPDH was used as an endogenous control. Experiment was done with the assistance of Shaad Hasim.

Chapter 4: Discussion

Lung cancer is a global health issue responsible for the majority of the cancer-related morbidities and mortalities worldwide [1,4]. NSCLC accounts for 85% of lung cancer diagnoses, and is often diagnosed at later stages of the disease due to the lack of effective screening methods [5,162]. Platin-based doublet chemotherapy is the standard treatment regimen used against advanced NSCLC, with cisplatin being commonly employed in this setting [36]. Agents used in combination with cisplatin include paclitaxel, docetaxel, and gemcitabine [16], however, these combinations have been determined empirically, without fully understanding their underlying mechanisms [145]. Furthermore, the use of cisplatin is limited due to toxic side effects as well as the development of resistance, thus many patients are exposed to it without receiving any clinical benefits [36,52]. This is further confirmed at the clinical level since the five-year survival rate of this disease is lower than other commonly diagnosed cancers [2]. Therefore, alternative rational therapeutic combinations against NSCLC are urgently required.

Previously our laboratory identified ATF3, an important regulator of cellular stress responses, as a target of cisplatin cytotoxicity, regulated mainly through the MAPK pathway [101]. In this study, the role of ATF3 as a novel therapeutic target in cisplatin cytotoxicity was further investigated using various *in vitro* cellular models including wild type and ATF3-/- MEFs as well as NSCLC cell lines Calu6 and H23, and their cisplatin-resistant sub-lines, Calu6cisR1 and H23cisR1, which were previously developed in our laboratory. There are various cellular pathways activated by cisplatin, leading to DNA damage and the production of ROS, which are known to induce ATF3 [84,129,163]. The

role of ROS, DDR, specifically the ATM kinase, and the MAPK pathway, specifically the JNK component, in cisplatin's induction of ATF3 were evaluated by employing specific inhibitors in NSCLC cell lines. Furthermore, vorinostat and topotecan were evaluated as enhancers of cisplatin cytotoxicity and ATF3 inducers, following their identification from a 1200 FDA approved library screen. Both compounds enhanced cisplatin cytotoxicity in both parental and cisR1 sub-lines. Furthermore, the level of ATF3 expression was enhanced following the combination of cisplatin with either vorinostat or topotecan, compared to each agent alone in the cisR1 cells, suggesting that ATF3 could have a role in overcoming cisplatin resistance. Finally, ATF3 expression was evaluated in *ex vivo* patient lung tumors and their adjacent normal tissues following treatment with cisplatin. The approach of identifying ATF3 expression using RT-qPCR was determined to be feasible as none of the normal tissue evaluated displayed ATF3 expression, while three of the six lung tumors displayed increase levels of ATF3 expression. Overall, this study highlights ATF3's potential role in cisplatin resistance as well as its potential to be targeted to enhance cisplatin cytotoxicity in resistant disease.

4.1. ATF3's role in cisplatin cytotoxicity

In order to be able to identify more rational combination therapies against NSCLC, it is important to understand the mechanisms underlying cisplatin's cytotoxicity. Our laboratory has previously identified ATF3, a stress inducible gene, as a key player in cisplatin cytotoxicity in various cancer cell lines [101]. The role of ATF3 in platin cytotoxicity was further confirmed in this study using wild type and ATF3-/- MEFs, where the ATF3-/- MEFs displayed less sensitivity to platins compared to their wild type counterparts. Importantly, no difference in cytotoxicity was observed in wild type and

ATF3-/- MEFs following treatment with docetaxel, a tubulin stabilizer [153]. The knockdown of ATF3 in the NSCLC cell line A549 has previously been shown to reduce sensitivity to cisplatin [101]. ATF3's role in both cell proliferation and apoptosis have been demonstrated in various studies [137,138]. However, the experiments and the cellular context used in this study further support ATF3 as a mediator of apoptosis as its absence decreased sensitivity to cisplatin. Overall, this suggests some specificity for ATF3 in regulating cisplatin-induced cytotoxicity. A knockout approach, such as the CRISPR/Cas9 system, employing NSCLC cell lines could further substantiate ATF3's role in cisplatin cytotoxicity in NSCLC as a future direction.

To further study the role of ATF3 in cisplatin resistance, our laboratory derived a variety of cisplatin-resistant sub-lines, including Calu6cisR1 and H23cisR1. ATF3 was identified as the most significantly differentially induced gene whose expression was abrogated in the Calu6cisR1 and H23cisR1 compared to their parental counterparts following cisplatin treatment. This further highlights ATF3's role in cisplatin resistance as the cisR1 sub-lines also displayed less sensitivity to cisplatin in comparison to the parental cell lines. Additionally, the activation of the MAPK component JNK was identified to be abrogated in the cisR1 sub-lines [104]. Although the pathways driving the induction of ATF3 expression following cisplatin treatment are abrogated in the cisplatin-resistant cell lines, the induction of ATF3 still occurred in these cells from other cellular pathways, suggesting a possible strategy to overcome cisplatin-resistance.

Our laboratory previously identified the components of the MAPK pathway as playing a role in cisplatin's induction of ATF3 [101], however, other mechanisms are also activated following treatment with cisplatin that have also been linked to the ATF3

induction. Cisplatin can cause oxidative stress in cells, which leads to the accumulation of ROS [84]. ATF3 can be induced by ATF4, a mediator of the ISR, whose induction can be induced by ROS [128]. NAC, a ROS scavenger, in combination with cisplatin inhibited cisplatin-induced ATF3 in NSCLC cells, which indicates that a pathway involving ROS is playing a role in cisplatin's induction of ATF3. Wu et al. have shown that NAC inhibits cisplatin's induction of the death receptor and mitochondrial apoptotic pathways [164]. The involvement of ROS in cisplatin cytotoxicity through the induction of ATF3 warrants further study. As previously discussed, activated cisplatin in the cell has an affinity for thiol-containing molecules, such as GSH [60]. NAC is a precursor for GSH, which suggests that pre-treatment with NAC results in increased intracellular levels of GSH, which could also bind with cisplatin [49,165]. This binding can limit the active cisplatin that is available to form DNA-adducts as the cisplatin-GSH compound tends to be exported from cells [72]. This could represent an alternative mechanism explaining the absence of ATF3 expression observed following treatment with NAC and cisplatin in the NSCLC cell lines. Evaluating the effect of cisplatin on cell viability in the presence and absence of NAC will also provide a more in depth understanding of role of ROS in cisplatin-induced cytotoxicity. Furthermore, MAPK signalling pathways have been linked to the regulation of cisplatin cytotoxicity as well as the induction of ATF3 [101,83]. The JNK pathway was previously determined to be abrogated in the Calu6cisR1 and H23cisR1 cell lines and the addition of a hyperactive JNK construct was able to enhance its sensitivity to cisplatin [104]. Additionally, the Calu6 cell lines were previously treated with cisplatin (1 and 4μg/mL) with and without SP600125, where a significant increase in viability was observed in the presence of the JNK inhibitor [104].

In this study, reduced ATF3 expression was observed with the JNK inhibitor, which is further suggesting a role for the MAPK signalling pathway in regulating cisplatin cytotoxicity and resistance that may be related to ATF3 expression.

4.2 Enhancing cisplatin cytotoxicity in combination with other ATF3 inducers

Our laboratory employed a library screen comprised of 1200 FDA approved compounds in order to identify 1) agents that enhance cisplatin cytotoxicity in the NSCLC cell line Calu6 and 2) agents that require functional ATF3 to induce cytotoxicity comparing wild type and ATF3-/- MEFs. Two candidates that were identified as hits in both screens were vorinostat and topotecan.

Vorinostat is a HDAC inhibitor that targets class I and II HDACs, which are zinc-binding enzymes [149]. Vorinostat is considered to be a pan-HDAC inhibitor due to the fact that it targets more than one class of HDACs [149]. HDACs are responsible for catalyzing the removal of acetyl groups from histones, which results in transcriptional repression [147]. Vorinostat inhibits these enzymes by binding to the zinc atom that is located on the catalytic site of the HDACs, resulting in an accumulation of acetylated proteins, including histones [147]. The aberrant expression and activity of HDACs have been identified in a number of cancers, including solid tumors [149,166]. Therefore, HDAC inhibitors, including vorinostat, have generally been associated with anticancer activity by inducing apoptosis and cell cycle arrest, as well as interfering with angiogenesis [146]. Furthermore, vorinostat has been FDA approved for the treatment of cutaneous T cell lymphoma and is in clinical trials for use as both monotherapy and combination therapy with other anticancer agents [149,150]. The mechanisms underlying vorinostat's mode of action are not completely understood, however, treatment with

vorinostat has been shown to selectively alter 2-10% of gene expression through upregulation as well as downregulation [149]. In a study by Wilson et al., ATF3 was shown to be induced by HDAC inhibitors in a panel of colon cancer cell lines [167]. Furthermore, our laboratory previously established ATF3 as a target of M344, an HDAC inhibitor, in various human cancer lines [126].

In this study, vorinostat was evaluated as a single agent as well as in combination with cisplatin against NSCLC. Differential sensitivity was observed between the wild type and ATF3-/- MEFs as well as between the parental Calu6 and H23 and their cisplatin-resistant counterparts, Calu6cisR1 and H23cisR1 following MTT assays, confirming the role of ATF3 in vorinostat cytotoxicity. ATF3 induction was abrogated in the cisR1 sub-lines compared to their parental cell lines, thus further suggesting a role for ATF3 in the differential cytotoxicity observed. Importantly, combinations of vorinostat and cisplatin generally induced a synergistic cytotoxic response in both the parental and their cisplatin resistant sub-lines. Our laboratory has previously showed that the HDAC inhibitor M344 enhanced cisplatin cytotoxicity in ovarian and breast cancer cells [126]. Additionally, vorinostat has also been shown to enhance cisplatin-induced apoptosis in SCLC cells [168].

The other agent that was identified as a hit from the library screens performed was topotecan. Topotecan, also known as Hycamtin, is topoisomerase inhibitor that has also been FDA approved as a chemotherapeutic agent for a variety of cancers, including ovarian and small-cell lung cancer [151,169]. Topotecan's interference between the topoisomerase I enzyme and DNA results in irreversible DSBs, which leads the cell towards apoptosis [152]. A synergistic interaction has been previously been observed

with the combination of cisplatin and topotecan in primary cultures of human tumor cells of different diagnoses [170]. Differential sensitivity was similarly observed between wild type and ATF3-/- MEFs, suggesting a role for ATF3 in regulating topotecan-induced cytotoxicity. Both parental and cisplatin-resistant cell lines displayed sensitivity to topotecan. While there was a statistically significant difference between the parental and resistant cell lines at lower concentrations, the difference in cell viability was modest as both cell lines displayed relatively high levels of cell death. However, the combination of these two agents displayed enhanced ATF3 expression compared to cisplatin and topotecan alone, which was also observed with the cisplatin and vorinostat combination. This suggests a role for ATF3 in overcoming cisplatin resistance.

Overall, the combination of cisplatin with vorinostat and topotecan provides evidence in support of the hypothesis that combining two agents that induce ATF3 through different pathways that induces synergistic or enhanced cytotoxicity may present a rational combination therapeutic approach. Additionally, several cellular signalling pathways, specifically ROS, MAPK pathway and the DDR, which could potentially be underlying vorinostat and topotecan's induction of ATF3 expression, were evaluated (Supplemental Figures 1-4). It would be of interest in the future to delineate the mechanisms that result in the enhanced ATF3 expression and synergy following the combination of cisplatin with vorinostat and topotecan.

The cytotoxic effects of the various agents used throughout this thesis, mainly cisplatin, vorinostat and topotecan, were evaluated using the MTT cell viability assay. MTT is a colorimetric assay that is commonly employed to screen cell viability following drug treatments [140]. However, a limitation associated with MTT assays is that the

readout obtained is based on the metabolic activity of the cells [140]. Thus, compounds affecting the metabolism of the cell, such as ROS production, could result in variant measures of cell viability. Therefore, PARP cleavage was also evaluated by Western blot analysis as another measure of apoptosis in cells, as it is a commonly employed marker of apoptosis [156]. An alternative to the MTT assay is the trypan blue exclusion assay, which measures cell viability on the basis of the permeability of their cell membrane, rather than metabolic activity [171].

4.3 ATF3 expression in NSCLC patient tumor samples

Resistance limits the use of cisplatin in the clinical setting [36]. Approximately 30-50% of patients display intrinsic resistance to platins [172], therefore, large number of patients are exposed to the toxicities of this agent without clinical benefits. Therefore, identifying predictive biomarkers for patient's response to platins is an ideal strategy in order to provide the best treatment approach for patients. Currently, targeted therapies are being employed in NSCLC, against tumors with predictive markers, such as EGFR mutations and ALK rearrangements [173,174]. The presence of EGFR mutations acts as a predictor of response to EGFR TKIs, which have displayed efficacy as a first-line treatment for NSCLC patients [24]. Additionally, the presence of ALK rearrangement in NSCLC patients can also be used as a predictor of response to ALK inhibitors [31]. However, patients with EGFR mutations and ALK rearrangements represent a small portion of NSCLC patients, therefore platins continue to be used as a standard treatment regimen against NSCLC [25,36]. Therefore, the identification of a marker that can predict response to platins presents an ideal strategy to identify patients that are sensitive and will receive its clinical benefits, as well as those who are resistant.

Our laboratory identified ATF3 as a gene that is differentially induced between parental and cisplatin-resistant cell lines. Following cisplatin treatment, ATF3 was induced in 3 of 6 NSCLC tumors that were surgically excised from patients underdoing lobectomy. No ATF3 induction was observed in the adjacent normal lung tissue. Taking the differential ATF3 induction observed in cisplatin resistant sub-lines along with its induction in NSCLC *ex* vivo tissue, the induction of ATF3 may represent a biomarker of response to cisplatin that can be evaluated in *ex-vivo* patient samples that may be employed if warranted by future studies to inform treatment options in NSCLC patients.

4.4 Conclusions

Cisplatin resistance plays a significant role in limiting the utilization of this important therapeutic agent in NSCLC patients [80]. Delineating the mechanisms underlying cisplatin resistance will provide therapeutic options to overcome this resistance and provide more refined therapeutic options in a clinical setting. In this study, we established ATF3 as a key regulator of cisplatin-induced cytotoxicity and therapeutic target in NSCLC cell lines whose induction is abrogated in resistant cells. We further provide evidence that combining inducers of ATF3, specifically vorinostat and topotecan, with cisplatin will not only enhance its cytotoxicity, but may potentially help alleviate cisplatin resistance in NSCLC. ATF3 expression induced by cisplatin, vorinostat and topotecan suggested roles for ROS, DDR (ATM), and JNK pathways. These results also suggest a novel therapeutic strategy of combining inducers of ATF3 expression to drive tumor cell apoptosis that requires further study. Finally, ATF3 may represent a predictor of platin response, which should be further evaluated in patients undergoing a platin treatment.

CONTRIBUTIONS

- The library screen done in the Calu6 cell line (Table 1.1a) was performed by Stefanie Reid.
- The library screen done in the MEFs (Table 1.1b) presented in the supplemental data was performed by Mohamed Shaad Hasim.
- The RT-qPCR for the *ex vivo* lung samples (Figure 3.14) was performed with the assistance of Mohamed Shaad Hasim.

REFERENCES

1. Ferlay J, Soerjomataram I, Dikshit R, et al. Cancer incidence and mortality worldwide: Sources, methods and major patterns in GLOBOCAN 2012. *Int J Cancer*. 2015;136(5):E359-E386.

2. Canadian Cancer Society's Advisory Committee on Cancer Statistics. *Canadian Cancer Statistics 2017*.; 2017.

3. Witschi H. A short history of lung cancer. *Toxicol Sci*. 2001;64(1):4-6.

4. Ridge CA, McErlean AM, Ginsberg MS. Epidemiology of Lung Cancer. *Semin Intervent Radiol*. 2013;30:93-98.

5. Herbst RS, Heymach J V., Lippman SM. Lung cancer. *N Engl J Med*. 2008;359(13):1367-1380.

6. Zappa C, Mousa SA. Non-small cell lung cancer: current treatment and future advances. *Transl Lung Cancer Res*. 2016;5(3):288-300.

7. Devesa SS, Bray F, Vizcaino AP, Parkin DM. International lung cancer trends by histologic type: Male:female differences diminishing and adenocarcinoma rates rising. *Int J Cancer*. 2005;117(2):294-299.

8. Sun S, Schiller JH, Gazdar AF. Lung cancer in never smokers - A different disease. *Nat Rev Cancer*. 2007;7(10):778-790.

9. Morabia a, Wynder EL. Cigarette smoking and lung cancer cell types. *Cancer*. 1991;68(9):2074-2078.

10. Khuder SA. Effect of cigarette smoking on major histological types of lung cancer: A meta-analysis. *Lung Cancer*. 2001;31(2-3):139-148.

11. Sholl LM. Large-cell carcinoma of the lung: A diagnostic category redefined by immunohistochemistry and genomics. *Curr Opin Pulm Med*. 2014;20(4):324-331.

12. Muscat JE, Stellman SD, Zhang ZF, Neugut… AI. Cigarette smoking and large cell carcinoma of the lung. ... *Biomarkers Prev*. 1997;6(July):477-480.

13. Islami F, Torre LA, Jemal A. Global trends of lung cancer mortality and smoking prevalence. *Transl lung cancer Res*. 2015;4(4):327-338.

14. Proctor RN. The history of the discovery of the cigaretteelung cancer link: Evidentiary traditions, corporate denial, global toll. *Tob Control*. 2012;21(2):87-91.

15. Hecht SS. Tobacco smoke carcinogens and lung cancer. *Curr Cancer Res*. 2011;6:53-74.

16. Molina JR, Yang P, Cassivi SD, Schild SE, Adjei AA. Non-small cell lung cancer: epidemiology, risk factors, treatment, and survivorship. *Mayo Clin Proc*. 2008;83(5):584-594.

17. Trédaniel J, Boffetta P, Saracci R, Hirsch A. Non-smoker lung cancer deaths attributable to exposure to spouse's environmental tobacco smoke. *Int J Epidemiol*. 1997;26(5):939-944.

18. Stayner L, Bena J, Sasco AJ, et al. Lung cancer risk and workplace exposure to environmental tobacco smoke. *Am J Public Health*. 2007;97(3):545-551.

19. Pope CA, Burnett RT, Thun MJ, et al. Lung cancer, cardiopulmonary mortality, and long-term exposure to fine particulate air pollution. *JAMA*. 2002;287(9):1132-1141.

20. Cohen AJ. Outdoor air pollution and lung cancer. *Environ Health Perspect*. 2000;108(SUPPL. 4):743-750.

21. Heintz NH, Janssen-Heininger YMW, Mossman BT. Asbestos, lung cancers, and mesotheliomas: From molecular approaches to targeting tumor survival pathways. *Am J Respir Cell Mol Biol*. 2010;42(2):133-139.

22. Lubin JH, Boice JD, Edling C, et al. Lung cancer in radon-exposed miners and estimation of risk from indoor exposure. *J Natl Cancer Inst*. 1995;87(11):817-827.

23. Kanwal M, Ding X-J, Cao Y. Familial risk for lung cancer. *Oncol Lett*. 2017;13(2):535-542.

24. Bethune G, Bethune D, Ridgway N, Xu Z. Epidermal growth factor receptor (EGFR) in lung cancer: An overview and update. *J Thorac Dis*. 2010;2(1):48-51.

25. Chan BA, Hughes BGM. Targeted therapy for non-small cell lung cancer: current standards and the promise of the future. *Transl lung cancer Res*. 2015;4(1):36-54.

26. Xu N, Fang W, Mu L, et al. Overexpression of wildtype EGFR is tumorigenic and denotes a therapeutic target in non-small cell lung cancer. *Oncotarget*. 2016;7(4):3884-3896.

27. Takahashi T, Nau M, Chiba I, et al. p53: a frequent target for genetic abnormalities in lung cancer. *Science (80-)*. 1989;246(4929):491-494.

28. Suzuki K, Matsubara H. Recent advances in p53 research and cancer treatment. *J Biomed Biotechnol*. 2011;2011:1-7.

29. Hwang SJ, Cheng LSC, Lozano G, Amos CI, Gu X, Strong LC. Lung cancer risk in germline p53 mutation carriers: Association between an inherited cancer predisposition, cigarette smoking, and cancer risk. *Hum Genet*. 2003;113(3):238-243.

30. Bergethon K, Shaw AT, Ou SHI, et al. ROS1 rearrangements define a unique molecular class of lung cancers. *J Clin Oncol*. 2012;30(8):863-870.

31. Shackelford RE, Vora M, Mayhall K, Cotelingam J. ALK-rearrangements and testing methods in non-small cell lung cancer: a review. *Genes Cancer*. 2014;5(1-2):1-14.

32. Uramoto H, Tanaka F. Recurrence after surgery in patients with NSCLC. *Transl Lung Cancer Res*. 2014;3(4):242-249.

33. Wood AJJ, Ihde DC. Chemotherapy of Lung Cancer. *N Engl J Med*. 1992;327(20):1434-1441.

34. Artal Cortés Á, Calera Urquizu L, Hernando Cubero J. Adjuvant chemotherapy in non-small cell lung cancer: state-of-the-art. *Transl lung cancer Res*. 2015;4(2):191-197.

35. Non-small Cell Lung Cancer Collaborative Group. Chemotherapy in non-small cell lung cancer: a meta-analysis using updated data on individual patients from 52 randomised clinical trials. Non-small Cell Lung Cancer Collaborative Group. *BMJ*. 1995;311(7010):899-909.

36. Dasari S, Bernard Tchounwou P. Cisplatin in cancer therapy: Molecular mechanisms of action. *Eur J Pharmacol*. 2014;740:364-378.

37. Di Maio M, Chiodini P, Georgoulias V, et al. Meta-analysis of single-agent chemotherapy compared with combination chemotherapy as second-line treatment of advanced non-small-cell lung cancer. *J Clin Oncol*. 2009;27(11):1836-1843.

38. Group NMC. Chemotherapy in addition to supportive care improves survival in advanced non-small-cell lung cancer: a systematic review and meta-analysis of individual patient data from 16 randomized controlled trials. *J Clin Oncol*. 2008;26(28):4617-4625.

39. Saadeddin A. Radiotherapy for NSCLC: Review of conventional and new treatment techniques. *J Infect Public Health*. 2012;5(5 SUPPL.1).

40. Wolf J, Patno ME, Roswit B, D'Esopo N. Controlled Study of Survival of Patients with Clinically Inoperable Lung Cancer Treated with Radiation Therapy. *Am J Med*. 1966;40:360-367.

41. Glatzer M, Elicin O, Ramella S, Nestle U, Putora PM. Radio(chemo)therapy in locally advanced nonsmall cell lung cancer. *Eur Respir Rev*. 2016;25(139):65-70.

42. Schaake-Koning C, van den Bogaert W, Dalesio O, et al. Effects of Concomitant Cisplatin and Radiotherapy on Inoperable Non-Small-Cell Lung Cancer. *N Engl J Med*. 1992;326(8):524-530.

43. Rosenberg B, Van Camp L, Krigas T. Inhibition of cell division in Escherichia coli by electrolysis products from a platinum electrode [17]. *Nature*. 1965;205(4972):698-699.

44. Rosenberg B, Van Camp L, Trosko JE, Mansour VH. Platinum compounds: a new class of potent antitumour agents. *Nature*. 1969;222(5191):385-386.

45. Kelland L. The resurgence of platinum-based cancer chemotherapy. *Nat Rev Cancer*. 2007;7(8):573-584.

46. Hess LM, Benham-Hutchins M, Herzog TJ, et al. A meta-analysis of the efficacy of intraperitoneal cisplatin for the front-line treatment of ovarian cancer. *Int J Gynecol Cancer*. 2007;17(3):561-570.

47. Rose PG, Bundy BN, Watkins EB, et al. Concurrent Cisplatin-Based Radiotherapy and Chemotherapy for Locally Advanced Cervical Cancer. *N Engl J Med*. 1999;340(15):1144-1153.

48. Herrera-Pérez Z, Gretz N, Dweep H. A Comprehensive Review on the Genetic Regulation of Cisplatin-induced Nephrotoxicity. *Curr Genomics*. 2016;17(3):279-293.

49. Siddik ZH. Cisplatin: Mode of cytotoxic action and molecular basis of resistance. *Oncogene*. 2003;22(47 REV. ISS. 6):7265-7279.

50. Wang D, Lippard SJ. Cellular processing of platinum anticancer drugs. *Nat Rev Drug Discov*. 2005;4(4):307-320.

51. Wheate NJ, Walker S, Craig GE, Oun R. The status of platinum anticancer drugs in the clinic and in clinical trials. *Dalt Trans*. 2010;39(35):8113.

52. Janku F, Stewart DJ, Kurzrock R. Targeted therapy in non-small-cell lung canceris it becoming a reality? *Nat Rev Clin Oncol*. 2010;7(7):401-414.

53. Florea A-M, Büsselberg D. Cisplatin as an Anti-Tumor Drug: Cellular Mechanisms of Activity, Drug Resistance and Induced Side Effects. *Cancers (Basel)*. 2011;3(4):1351-1371.

54. Miller RP, Tadagavadi RK, Ramesh G, Reeves WB. Mechanisms of cisplatin nephrotoxicity. *Toxins (Basel)*. 2010;2(11):2490-2518.

55. Mukhopadhyay P, Horváth B, Zsengellér Z, et al. Mitochondrial-targeted antioxidants represent a promising approach for prevention of cisplatin-induced nephropathy. *Free Radic Biol Med*. 2012;52(2):497-506.

56. de Sousa GF, Wlodarczyk SR, Monteiro G. Carboplatin: Molecular mechanisms of action associated with chemoresistance. *Brazilian J Pharm Sci*. 2014;50(4):693-702.

57. Ho GY, Woodward N, Coward JIG. Cisplatin versus carboplatin: Comparative review of therapeutic management in solid malignancies. *Crit Rev Oncol Hematol*. 2016;102:37-46.

58. de Castria TB, da Silva EMK, Gois AFT, Riera R. Cisplatin versus carboplatin in combination with third-generation drugs for advanced non-small cell lung cancer. *Cochrane Database Syst Rev*. 2013;2013(8).

59. Ardizzoni A, Boni L, Tiseo M, et al. Cisplatin- versus carboplatin-based chemotherapy in first-line treatment of advanced non-small-cell lung cancer: an individual patient data meta-analysis. *J Natl Cancer Inst*. 2007;99(11):847-857.

60. Galluzzi L, Senovilla L, Vitale I, et al. Molecular mechanisms of cisplatin resistance. *Oncogene*. 2012;31(15):1869-1883.

61. Wynne P, Newton C, Ledermann JA, Olaitan A, Mould TA, Hartley JA. Enhanced repair of DNA interstrand crosslinking in ovarian cancer cells from patients following treatment with platinum-based chemotherapy. *Br J Cancer*. 2007;97(7):927-933.

62. Lee J, Prohaska JR, Thiele DJ. Essential role for mammalian copper transporter Ctr1 in copper homeostasis and embryonic development. *Proc Natl Acad Sci*. 2001;98(12):6842-6847.

63. Holzer AK, Manorek GH, Howell SB. Contribution of the Major Copper Influx Transporter CTR1 to the Cellular Accumulation of Cisplatin, Carboplatin, and Oxaliplatin. *Mol Pharmacol*. 2006;70(4):1390-1394.

64. Holzer AK, Howell SB. The internalization and degradation of human copper transporter 1 following cisplatin exposure. *Cancer Res*. 2006;66(22):10944-10952.

65. Holzer AK, Katano K, Klomp LWJ, Howell SB. Cisplatin rapidly down-regulates its own influx transporter hCTR1 in cultured human ovarian carcinoma cells. *Clin Cancer Res*. 2004;10(19):6744-6749.

66. Borst P, Evers R, Kool M, Wijnholds J. A family of drug transporters: The multidrug resistance-associated proteins. *J Natl Cancer Inst*. 2000;92(16):1295-1302.

67. Cui Y, König J, Buchholz JK, Spring H, Leier I, Keppler D. Drug resistance and ATP-dependent conjugate transport mediated by the apical multidrug resistance protein, MRP2, permanently expressed in human and canine cells. *Mol Pharmacol*. 1999;55(5):929-937.

68. Komatsu M, Sumizawa T, Mutoh M, et al. Copper-transporting P-type adenosine triphosphatase (ATP7B) is associated with cisplatin resistance. *Cancer Res*. 2000;60(5):1312-1316.

69. Inoue Y, Matsumoto H, Yamada S, et al. Association of ATP7A expression and in vitro sensitivity to cisplatin in non-small cell lung cancer. *Oncol Lett*. 2010;1(5):837-840.

70. Nakayama K, Kanzaki A, Ogawa K, Miyazaki K, Neamati N, Takebayashi Y. Copper-transporting P-type adenosine triphosphatase (ATP7B) as a cisplatin based chemoresistance marker in ovarian carcinoma: Comparative analysis with expression of MDR1, MRP1, MRP2, LRP and BCRP. *Int J Cancer*. 2002;101(5):488-495.

71. Godwin AK, Meister A, O'Dwyer PJ, Huang CS, Hamilton TC, Anderson ME. High resistance to cisplatin in human ovarian cancer cell lines is associated with marked increase of glutathione synthesis. *Proc Natl Acad Sci U S A*. 1992;89(7):3070-3074.

72. Ishikawa T. The ATP-dependent glutathione S-conjugate export pump. *Trends Biochem Sci*. 1992;17(11):463-468.

73. Selvakumaran M, Pisarcik D a, Bao R. Enhanced Cisplatin Cytotoxicity by Disturbing the Nucleotide Excision Repair Pathway in Ovarian Cancer Cell Lines. *Cancer Res*. 2003;63:1311-1316.

74. Rosell R, Taron M, Barnadas A, Scagliotti G, Sarries C, Roig B. Nucleotide excision repair pathways involved in Cisplatin resistance in non-small-cell lung cancer. *Cancer Control*. 2003;10:297-305.

75. Olaussen KA, Dunant A, Fouret P, et al. DNA Repair by ERCC1 in Non–Small-Cell Lung Cancer and Cisplatin-Based Adjuvant Chemotherapy. *N Engl J Med*. 2006;355(10):983-991.

76. Jun HJ, Ahn MJ, Kim HS, et al. ERCC1 expression as a predictive marker of squamous cell carcinoma of the head and neck treated with cisplatin-based concurrent chemoradiation. *Br J Cancer*. 2008;99(1):167-172.

77. Usanova S, Piée-Staffa A, Sied U, et al. Cisplatin sensitivity of testis tumour cells is due to deficiency in interstrand-crosslink repair and low ercc1-xpf expression. *J Urol*. 2011;186(2):457.

78. Li G-M. Mechanisms and functions of DNA mismatch repair. *Cell Res*. 2008;18(1):85-98.

79. Sedletska Y, Giraud-Panis M-J, Malinge J-M. Cisplatin Is a DNA-Damaging Antitumour Compound Triggering Multifactorial Biochemical Responses in Cancer Cells: Importance of Apoptotic Pathways. *Curr Med Chem Agents*. 2005;5(3):251-265.

80. Köberle B, Tomicic MT, Usanova S, Kaina B. Cisplatin resistance: Preclinical findings and clinical implications. *Biochim Biophys Acta - Rev Cancer*. 2010;1806(2):172-182.

81. Vaisman A, Masutani C, Hanaoka F, Chaney SG. Efficient translesion replication past oxaliplatin and cisplatin GpG adducts by human DNA polymerase η. *Biochemistry*. 2000;39(16):4575-4580.

82. Reinhardt HC, Schumacher B. The p53 network: Cellular and systemic DNA damage responses in aging and cancer. *Trends Genet*. 2012;28(3):128-136.

83. Brozovic A, Osmak M. Activation of mitogen-activated protein kinases by cisplatin and their role in cisplatin-resistance. *Cancer Lett*. 2007;251(1):1-16.

84. Brozovic A, Ambriović-Ristov A, Osmak M. The relationship between cisplatin-Induced reactive oxygen species, glutathione, and BCL-2 and resistance to cisplatin. *Crit Rev Toxicol*. 2010;40(4):347-359.

85. Gadducci A, Cosio S, Muraca S, Genazzani AR. Molecular mechanisms of apoptosis and chemosensitivity to platinum and paclitaxel in ovarian cancer: Biological data and clinical implications. *Eur J Gynaecol Oncol*. 2002;23(5):390-396.

86. Horwich A, Shipley J, Huddart R. Testicular germ-cell cancer. In: *Lancet*. Vol 367. ; 2006:754-765.

87. Peng HQ, Hogg D, Malkin D, et al. Mutations of the p53 gene do not occur in testis cancer. *Cancer Res*. 1993;53(15):3574-3578.

88. De Feudis P, Debernardis D, Beccaglia P, et al. DDP-induced cytotoxicity is not influenced by p53 in nine human ovarian cancer cell lines with different p53 status. *Br J Cancer*. 1997;76(4):474-479.

89. Burger H, Nooter K, Boersma a W, Kortland CJ, Stoter G. Lack of correlation between cisplatin-induced apoptosis, p53 status and expression of Bcl-2 family proteins in testicular germ cell tumour cell lines. *Int J Cancer*. 1997;73(4):592-599.

90. Ahmad S. Platinum-DNA interactions and subsequent cellular processes controlling sensitivity to anticancer platinum complexes. *Chem Biodivers*. 2010;7(3):543-566.

91. Zhang W, Liu HT, Tu LIU H. MAPK signal pathways in the regulation of cell proliferation in mammalian cells. *Cell Res*. 2002;12(1):9-18.

92. Losa JH, Cobo CP, Viniegra JG, Sánchez-Arevalo Lobo VJ, Ramón y Cajal S, Sánchez-Prieto R. Role of the p38 MAPK pathway in cisplatin-based therapy. *Oncogene*. 2003;22(26):3998-4006.

93. Olson JM, Hallahan AR. p38 MAP kinase: A convergence point in cancer therapy. *Trends Mol Med*. 2004;10(3):125-129. doi:10.1016/j.molmed.2004.01.007.

94. Williams J, Lucas PC, Griffith KA, et al. Expression of Bcl-xL in ovarian carcinoma is associated with chemoresistance and recurrent disease. *Gynecol Oncol*. 2005;96(2):287-295.

95. Han J-Y, Hong EK, Choi BG, et al. Death Receptor 5 and Bcl-2 Protein Expression as Predictors of Tumor Response to Gemcitabine and Cisplatin in Patients with Advanced Non-Small-Cell Lung Cancer. *Med Oncol*. 2003;20(4):355-362.

96. Zhu S, Pabla N, Tang C, He L, Dong Z. DNA damage response in cisplatin-induced nephrotoxicity. *Arch Toxicol*. 2015;89(12):2197-2205.

97. Sirbu BM, Cortez D. DNA damage response: three levels of DNA repair regulation. *Cold Spring Harb Perspect Biol*. 2013;5(8):a012724.

98. Lovejoy CA, Cortez D. Common mechanisms of PIKK regulation. *DNA Repair (Amst)*. 2009;8(9):1004-1008.

99. Lavin MF, Gueven N. The complexity of p53 stabilization and activation. *Cell Death Differ*. 2006;13(6):941-950. doi:10.1038/sj.cdd.4401925.

100. Burger H, Nooter K, Boersma AWM, et al. Distinct p53-independent apoptotic cell death signalling pathways in testicular germ cell tumour cell lines. *Int J Cancer*. 1999;81(4):620-628.

101. St. Germain C, Niknejad N, Ma L, Garbuio K, Hai T, Dimitroulakos J. Cisplatin Induces Cytotoxicity through the Mitogen-Activated Protein Kinase Pathways and Activating Transcription Factor 3. *Neoplasia*. 2010;12(7):527-538.

102. Persons DL, Yazlovitskaya EM, Pelling JC. Effect of extracellular signal-regulated kinase on p53 accumulation in response to cisplatin. *J Biol Chem*. 2000;275(46):35778-35785.

103. Yan D, An G, Kuo MT. C-Jun N-terminal kinase signalling pathway in response to cisplatin. *J Cell Mol Med*. 2016;20(11):2013.

104. Bar J, Hasim MS, Baghai T, et al. Induction of Activating Transcription Factor 3 Is Associated with Cisplatin Responsiveness in Non–Small Cell Lung Carcinoma Cells. *Neoplasia*. 2016;18(9):525-535.

105. Berndtsson M, Hägg M, Panaretakis T, Havelka AM, Shoshan MC, Linder S. Acute apoptosis by cisplatin requires induction of reactive oxygen species but is not associated with damage to nuclear DNA. *Int J Cancer*. 2007;120(1):175-180.

106. Marullo R, Werner E, Degtyareva N, et al. Cisplatin induces a mitochondrial-ros response that contributes to cytotoxicity depending on mitochondrial redox status and bioenergetic functions. *PLoS One*. 2013;8(11).

107. Choi YM, Kim HK, Shim W, et al. Mechanism of cisplatin-induced cytotoxicity is correlated to impaired metabolism due to mitochondrial ROS generation. *PLoS One*. 2015;10(8).

108. Schweyer S, Soruri A, Heintze A, Radzun HJ, Fayyazi A. The role of reactive oxygen species in cisplatin-induced apoptosis in human malignant testicular germ cell lines. *Int J Oncol*. 2004;25(6):1671-1676.

109. Liu L, Wise DR, Diehl JA, Simon MC. Hypoxic reactive oxygen species regulate the integrated stress response and cell survival. *J Biol Chem*. 2008;283(45):31153-31162.

110. Pakos‐Zebrucka K, Koryga I, Mnich K, Ljujic M, Samali A, Gorman AM. The integrated stress response. *EMBO Rep*. 2016;17(10):1374-1395.

111. Yan C, Boyd DD. ATF3 regulates the stability of p53: A link to cancer. *Cell Cycle*. 2006;5(9):926-929.

112. Liang G, Wolfgang CD, Chen BPC, Chen TH, Hai T. ATF3 gene: Genomic organization, promoter, and regulation. *J Biol Chem*. 1996;271(3):1695-1701.

113. Chen BP, Liang G, Whelan J, Hai T. ATF3 and ATF3 delta Zip. Transcriptional repression versus activation by alternatively spliced isoforms. *J Biol Chem*. 1994;269(22):15819-15826.

114. Hashimoto Y, Zhang C, Kawauchi J, et al. An alternatively spliced isoform of transcriptional repressor ATF3 and its induction by stress stimuli. *Nucleic Acids Res*. 2002;30(11):2398-2406.

115. Shaulian E, Karin M. AP-1 in cell proliferation and survival. *Oncogene*. 2001;20(19 REV. ISS. 2):2390-2400. doi:10.1038/sj.onc.1204383.
116. Thompson MR, Xu D, Williams BRG. ATF3 transcription factor and its emerging roles in immunity and cancer. *J Mol Med*. 2009;87(11):1053-1060.

117. Hai T, Wolfgang CD, Marsee DK, Allen AE, Sivaprasad U. ATF3 and stress responses. In: *Gene Expression*. Vol 7. ; 1999:321-335.

118. Hsu JC, Bravo R, Taub R. Interactions among LRF-1, JunB, c-Jun, and c-Fos define a regulatory program in the G1 phase of liver regeneration. *Mol Cell Biol*. 1992;12(10):4654-4665.

119. Chen BP, Wolfgang CD, Hai T. Analysis of ATF3, a transcription factor induced by physiological stresses and modulated by gadd153/Chop10. *Mol Cell Biol*. 1996;16(3):1157-1168.

120. Fan F, Jin S, Amundson SA, et al. ATF3 induction following DNA damage is regulated by distinct signaling pathways and over-expression of ATF3 protein suppresses cells growth. *Oncogene*. 2002;21(49):7488-7496.

121. Nobori K, Ito H, Tamamori-Adachi M, et al. ATF3 inhibits doxorubicin-induced apoptosis in cardiac myocytes: A novel cardioprotective role of ATF3. *J Mol Cell Cardiol*. 2002;34(10):1387-1397.

122. Jiang H-Y, Wek S a, McGrath BC, et al. Activating transcription factor 3 is integral to the eukaryotic initiation factor 2 kinase stress response. *Mol Cell Biol*. 2004;24(3):1365-1377.

123. Yoshida T, Sugiura H, Mitobe M, et al. ATF3 Protects against Renal Ischemia-Reperfusion Injury. *J Am Soc Nephrol*. 2008;19(2):217-224.

124. Zimmermann J, Erdmann D, Lalande I, Grossenbacher R, Noorani M, Fürst P. Proteasome inhibitor induced gene expression profiles reveal overexpression of transcriptional regulators ATF3, GADD153 and MAD1. *Oncogene*. 2000;19(25):2913-2920.

125. Niknejad N, Morley M, Dimitroulakos J. Activation of the integrated stress response regulates lovastatin-induced apoptosis. *J Biol Chem*. 2007;282(41):29748-29756.

126. St Germain C, O'Brien A, Dimitroulakos J. Activating Transcription Factor 3 regulates in part the enhanced tumour cell cytotoxicity of the histone deacetylase inhibitor M344 and cisplatin in combination. *Cancer Cell Int*. 2010;10.

127. Lu D, Chen J, Hai T. The regulation of ATF3 gene expression by mitogen-activated protein kinases. *Biochem J*. 2007;401(2):559-567.

128. Wek RC, Jiang H-Y, Anthony TG. Coping with stress: eIF2 kinases and translational control. *Biochem Soc Trans*. 2006;34(1):7.

129. Zhang C, Gao C, Kawauchi J, Hashimoto Y, Tsuchida N, Kitajima S. Transcriptional activation of the human stress-inducible transcriptional repressor ATF3 gene promoter by p53. *Biochem Biophys Res Commun*. 2002;297(5):1302-1310.

130. Wei S, Wang H, Lu C, et al. The activating transcription factor 3 protein suppresses the oncogenic function of mutant p53 proteins. *J Biol Chem*. 2014;289(13):8947-8959.

131. Yan C, Lu D, Hai T, Boyd DD. Activating transcription factor 3, a stress sensor, activates p53 by blocking its ubiquitination. *EMBO J*. 2005;24(13):2425-2435.

132. Lee SH, Bahn JH, Whitlock NC, Baek SJ. Activating transcription factor 2 (ATF2) controls tolfenamic acid-induced ATF3 expression via MAP kinase pathways. *Oncogene*. 2010;29(37):5182-5192.

133. Sharma K, Vu T-T, Cook W, et al. p53-independent Noxa induction by cisplatin is regulated by ATF3/ATF4 in head and neck squamous cell carcinoma cells. *Mol Oncol*. 2018:1-11.

134. Ghosh AP, Klocke BJ, Ballestas ME, Roth KA. CHOP potentially co-operates with FOXO3a in neuronal cells to regulate PUMA and BIM expression in response to ER stress. *PLoS One*. 2012;7(6).

135. Lu D, Wolfgang CD, Hai T. Activating transcription factor 3, a stress-inducible gene, suppresses ras-stimulated tumorigenesis. *J Biol Chem*. 2006;281(15):10473-10481.

136. Tamura K, Hua B, Adachi S, et al. Stress response gene ATF3 is a target of c-myc in serum-induced cell proliferation. *EMBO J*. 2005;24(14):2590-2601.

137. Yin X, DeWille JW, Hai T. A potential dichotomous role of ATF3, an adaptive-response gene, in cancer development. *Oncogene*. 2008;27(15):2118-2127.

138. Jiang X, Kim K-J, Ha T, Lee S-H. Potential Dual Role of Activating Transcription Factor 3 in Colorectal Cancer. *Anticancer Res*. 2016;36(2):509-516.

139. Bottone FG, Moon Y, Kim JS, Alston-Mills B, Ishibashi M, Eling TE. The anti-invasive activity of cyclooxygenase inhibitors is regulated by the transcription factor ATF3 (activating transcription factor 3). *Mol Cancer Ther*. 2005;4(5):693-703.

140. Li X, Zhou X, Li Y, et al. Activating transcription factor 3 promotes malignance of lung cancer cells in vitro. *Thorac Cancer*. 2017;8(3):181-191.

141. Bandyopadhyay S, Wang Y, Zhan R, et al. The tumor metastasis suppressor gene Drg-1 down-regulates the expression of activating transcription factor 3 in prostate cancer. *Cancer Res*. 2006;66(24):11983-11990.

142. Frese S, Brunner T, Gugger M, Uduehi A, Schmid RA. Enhancement of Apo2L/TRAIL (tumor necrosis factor-related apoptosis-inducing ligand)-induced apoptosis in non-small cell lung cancer cell lines by chemotherapeutic agents without correlation to the expression level of cellular protease caspase-8 inhibitor. *J Thorac Cardiovasc Surg*. 2002;123(1):168-174.

143. Takahashi T, Carbone D, Takahashi T, et al. Wild-type but not mutant p53 suppresses the growth of human lung cancer cells bearing multiple genetic lesions. *Cancer Res*. 1992;52(8):2340-2343.

144. O'Brien A, Barber JEB, Reid S, Niknejad N, Dimitroulakos J. Enhancement of cisplatin cytotoxicity by disulfiram involves activating transcription factor 3. *Anticancer Res*. 2012;32(7):2679-2688.

145. Grossi F, Kubota K, Cappuzzo F, et al. Future scenarios for the treatment of advanced non-small cell lung cancer: focus on taxane-containing regimens. *Oncologist*. 2010;15(10):1102-1112.

146. Bubna A. Vorinostat-An overview. *Indian J Dermatol*. 2015;60(4):419.

147. Xu WS, Parmigiani RB, Marks PA. Histone deacetylase inhibitors: Molecular mechanisms of action. *Oncogene*. 2007;26(37):5541-5552.

148. Lee J-H, Choy ML, Ngo L, Foster SS, Marks P a. Histone deacetylase inhibitor induces DNA damage, which normal but not transformed cells can repair. *Proc Natl Acad Sci U S A*. 2010;107(33):14639-14644.

149. Marks PA, Breslow R. Dimethyl sulfoxide to vorinostat: Development of this histone deacetylase inhibitor as an anticancer drug. *Nat Biotechnol*. 2007;25(1):84-90.

150. Grant S, Easley C, Kirkpatrick P. Vorinostat. *Nat Rev Drug Discov*. 2007;6(1):21-22.

151. Heron JF. Topotecan: An Oncologist's View. *Oncologist*. 1998;3(6):390-402.
152. L.M. R-W, B.J. M. Topotecan in the management of cervical cancer. *Expert Opin Pharmacother*. 2007;8(2):227-236.

153. Stanton RA, Gernert KM, Nettles JH, Aneja R. Drugs that target dynamic microtubules: A new molecular perspective. *Med Res Rev*. 2011;31(3):443-481.

154. Hamdi M, Popeijus HE, Carlotti F, et al. ATF3 and Fra1 have opposite functions in JNK- and ERK-dependent DNA damage responses. *DNA Repair (Amst)*. 2008;7(3):487-496.

155. Zahr S, Mukhtar L, Dayekh K, et al. Inhibition of GGTase1 Enhances Erlotinib Efficacy in Squamous Cell Carcinoma Cells: Potential Novel Combination Therapeutic Approach. *Oncotarget (Under Revis*ion)

156. Kaufmann SH, Desnoyers S, Ottaviano Y, Davidson NE, Poirier GG. Specific Proteolytic Cleavage of Poly(ADP-ribose) Polymerase: An Early Marker of Chemotherapy-induced Apoptosis. *Cancer Res*. 1993;53(17):3976-3985.

157. Li Y, Yang D-Q. The ATM Inhibitor KU-55933 Suppresses Cell Proliferation and Induces Apoptosis by Blocking Akt In Cancer Cells with Overactivated Akt. *Mol Cancer Ther*. 2010;9(1):113-125.

158. Sánchez-Pérez I, Perona R. Lack of c-jun activity increases survival to cisplatin. *FEBS Lett*. 1999;453(1-2):151-158.

159. Potapova O, Basu S, Mercola D, Holbrook NJ. Protective role for c-Jun in the cellular response to DNA damage. *J Biol Chem*. 2001;276(30):28546-28553.

160. Musti AM, Treier M, Bohmann D. Reduced ubiquitin-dependent degradation of c-Jun after phosphorylation by map kinases. *Science (80-)*. 1997;275(5298):400-402.

161. Chou TC. Drug combination studies and their synergy quantification using the chou-talalay method. *Cancer Res*. 2010;70(2):440-446.

162. Hirsch FR, Franklin WA, Gazdar AF, Bunn PA. Early detection of lung cancer: clinical perspectives of recent advances in biology and radiology. *Clin Cancer Res*. 2001;7(1):5-22.

163. Edagawa M, Kawauchi J, Hirata M, et al. Role of Activating Transcription Factor 3 (ATF3) in Endoplasmic Reticulum (ER) stress-induced sensitization of p53-deficient human colon cancer cells to Tumor Necrosis Factor (TNF)-related apoptosis-inducing ligand (TRAIL)-mediated apoptosis through up-re. *J Biol Chem*. 2014;289(31):21544-21561.

164. Wu YJ, Muldoon LL, Neuwelt E a. The chemoprotective agent N-acetylcysteine blocks cisplatin-induced apoptosis through caspase signaling pathway. *J Pharmacol Exp Ther*. 2005;312(2):424-431.

165. Atkuri KR, Mantovani JJ, Herzenberg LA, Herzenberg LA. N-Acetylcysteine-a safe antidote for cysteine/glutathione deficiency. *Curr Opin Pharmacol*. 2007;7(4):355-359.

166. Özdağ H, Teschendorff AE, Ahmed AA, et al. Differential expression of selected histone modifier genes in human solid cancers. *BMC Genomics*. 2006;7.

167. Wilson AJ, Chueh AC, Tögel L, et al. Apoptotic sensitivity of colon cancer cells to histone deacetylase inhibitors is mediated by an Sp1/Sp3-activated transcriptional program involving immediate-early gene induction. *Cancer Res*. 2010;70(2):609-620.

168. Pan C-H, Chang Y-F, Lee M-S, et al. Vorinostat enhances the cisplatin-mediated anticancer effects in small cell lung cancer cells. *BMC Cancer*. 2016;16(1):857.

169. J. G. Safety of topotecan in the treatment of recurrent small-cell lung cancer and ovarian cancer. *Expert Opin Drug Saf*. 2007;6(1):53-62.

170. Jonsson E, Fridborg H, Nygren P, Larsson R. Synergistic interactions of combinations of topotecan with standard drugs in primary cultures of human tumor cells from patients. *Eur J Clin Pharmacol*. 1998;54(7):509-514.

171. Strober W. Trypan blue exclusion test of cell viability. *Curr Protoc Immunol*. 2001;Appendix 3:Appendix 3B. doi:10.1002/0471142735.ima03bs21.

172. Schiller JH, Harrington D, Belani CP, et al. Comparison of four chemotherapy regimens for advanced non-small-cell lung cancer. *N Engl J Med*. 2002;346(2):92-98.

173. Paez JG, Jänne PA, Lee JC, et al. EGFR mutations in lung cancer: correlation with clinical response to gefitinib therapy. *Science*. 2004;304(5676):1497-1500.

174. Aisner DL, Marshall CB. Molecular pathology of non-small cell lung cancer: A practical guide. *Am J Clin Pathol*. 2012;138(3):332-346.

Appendix: Supplementary Data

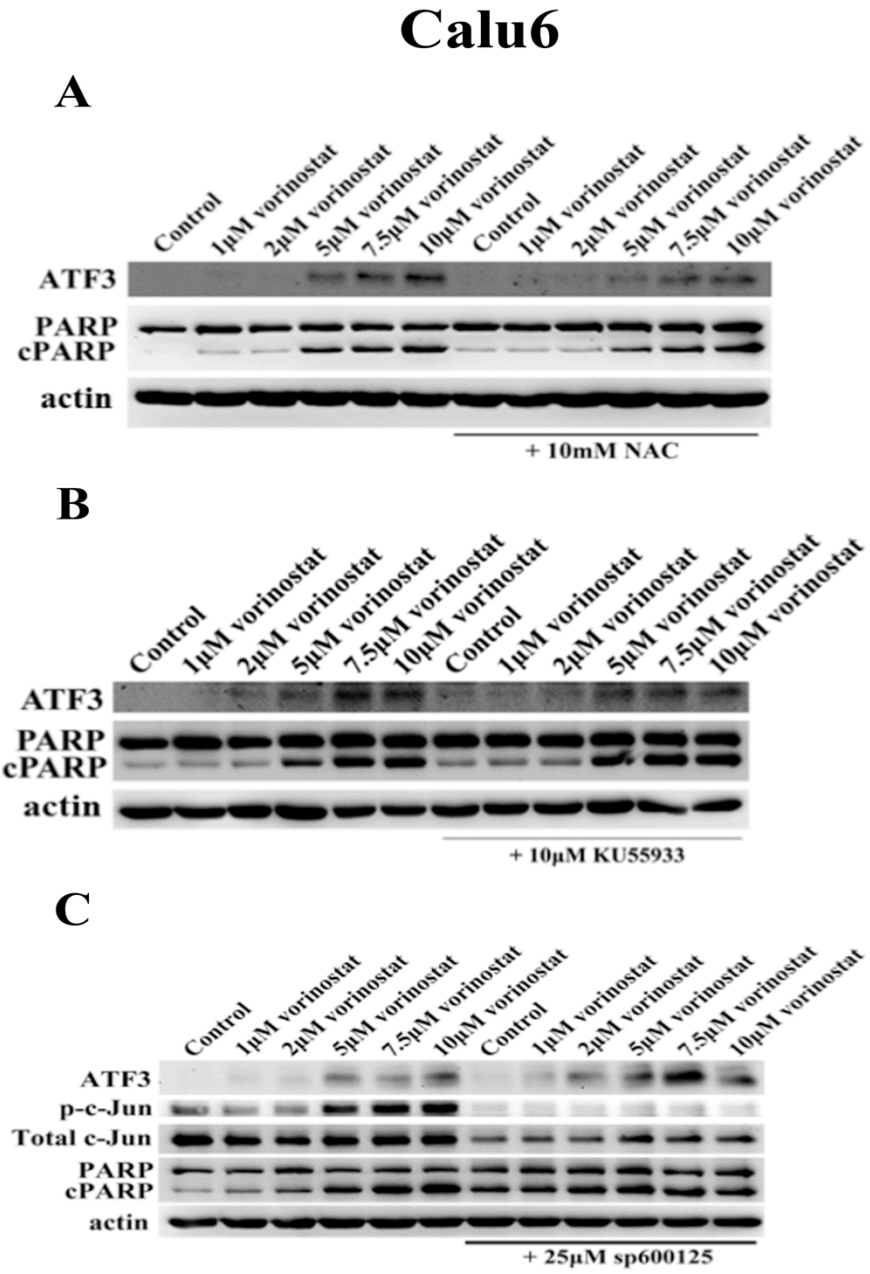

Supplemental Figure 1. Evaluating the pathways underlying vorinostat cytotoxicity in the Calu6 cell line. Calu6 cells were treated with **A)** 10mM NAC, **B)** 10μM ATM inhibitor KU55933 and **C)** 25μM JNK inhibitor SP600125 prior to co-treatment with vorinostat for 24 hours. Western blot analysis was performed to evaluate ATF3 expression and PARP cleavage. No pronounced attenuation in the ATF3 expression was observed following the co-treatment of vorinostat with NAC, KU55933 and SP600125. Actin was used as a loading control.

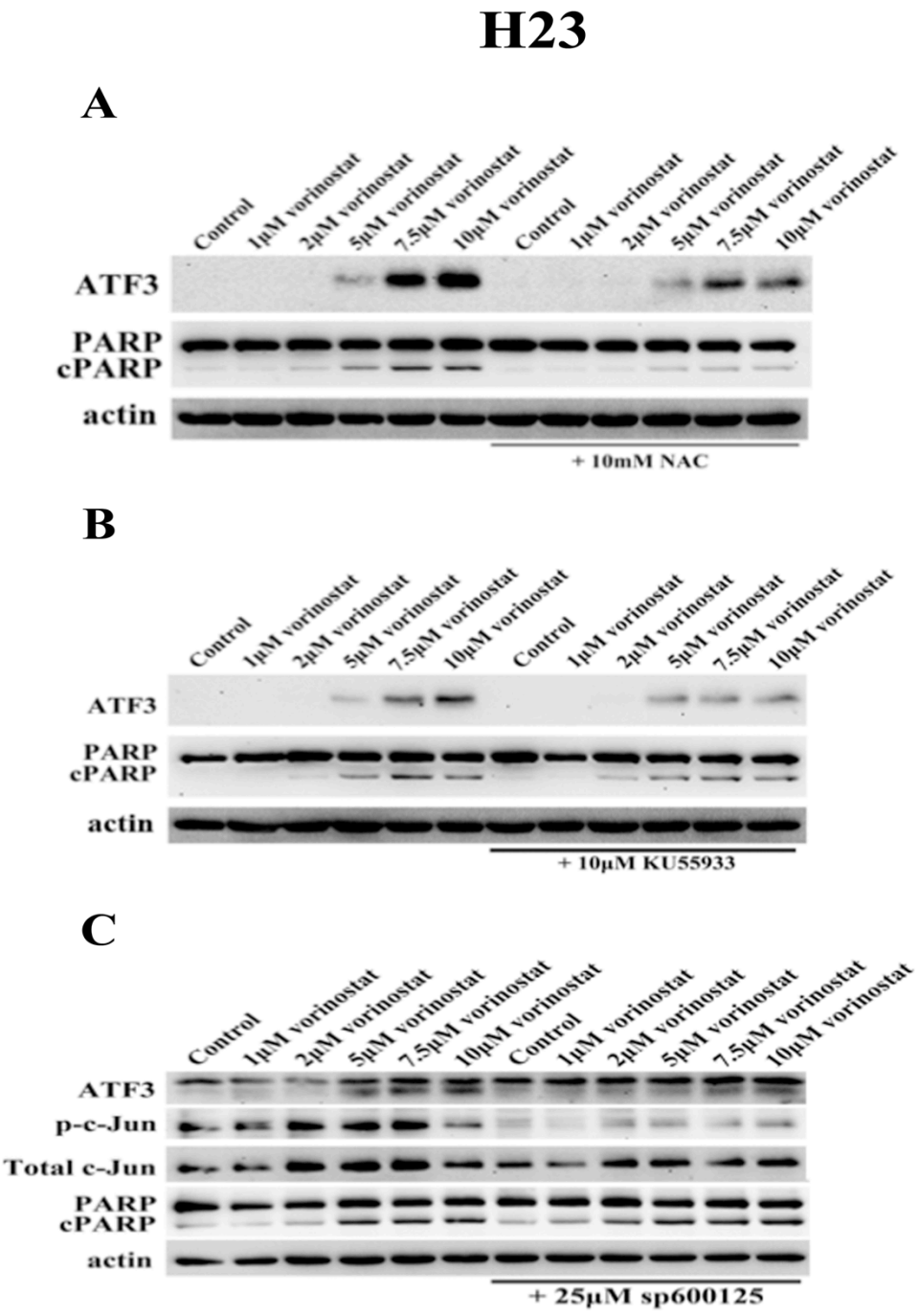

Supplemental Figure 2. Evaluating the pathways underlying vorinostat cytotoxicity in the H23 cell line. H23 cells were treated with **A)** 10mM NAC, **B)** 10μM ATM inhibitor KU55933 and **C)** 25μM JNK inhibitor SP600125 prior to co-treatment with vorinostat for 24 hours. Western blot analysis was performed to evaluate ATF3 expression and PARP cleavage. ATF3 expression was attenuated following in the presence of NAC and KU55933, while the attenuated was not as pronounced with SP600125. Actin was used as a loading control.

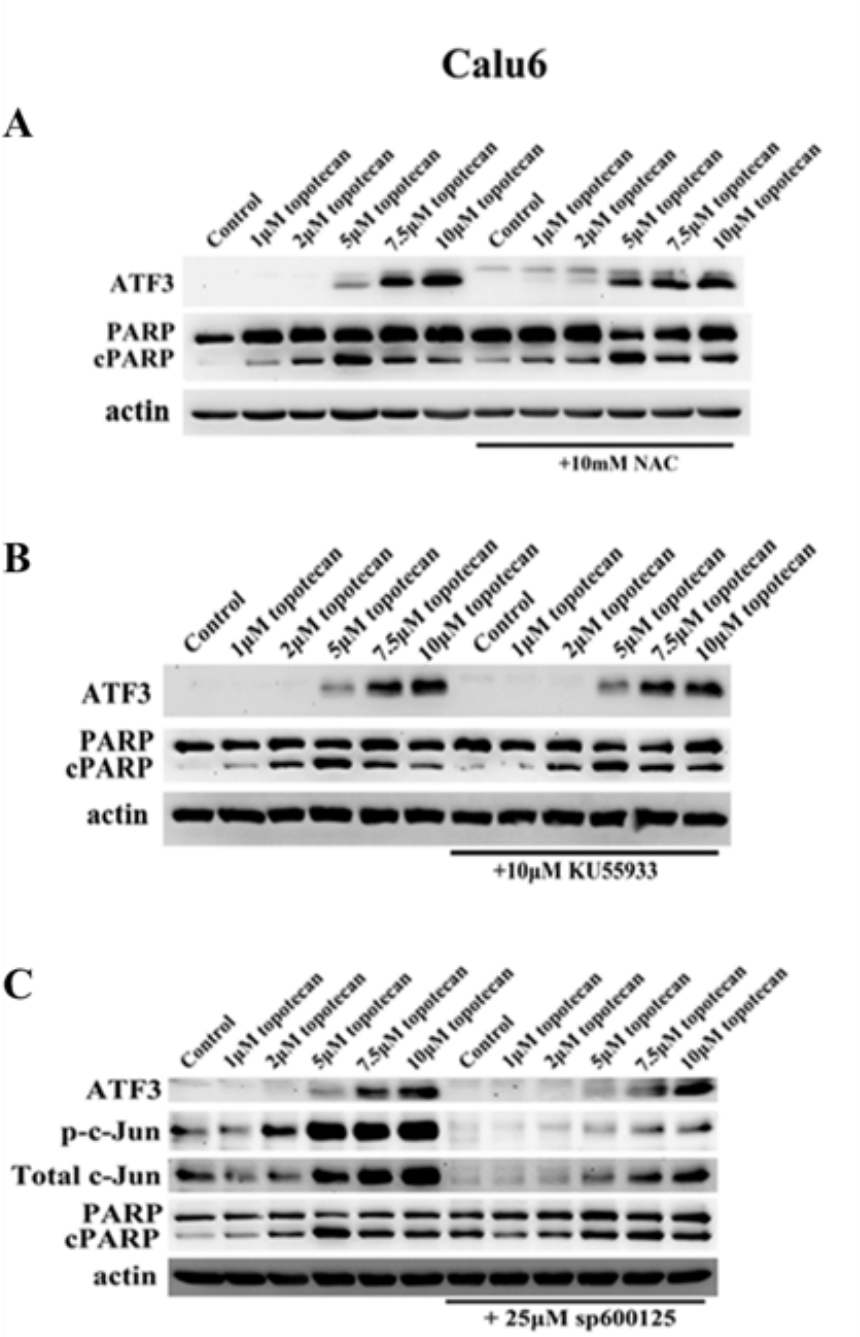

Supplemental Figure 3. Evaluating the pathways underlying topotecan cytotoxicity in the Calu6 cell line. Calu6 cells were treated with **A)** 10mM NAC, **B)** 10μM ATM inhibitor KU55933 and **C)** 25μM JNK inhibitor SP600125 prior to co-treatment with topotecan for 24 hours. Western blot analysis was performed to evaluate ATF3 expression and PARP cleavage. No pronounced attenuation in the ATF3 expression was observed following the co-treatment of topotecan with NAC, KU55933 and SP600125. Actin was used as a loading control.

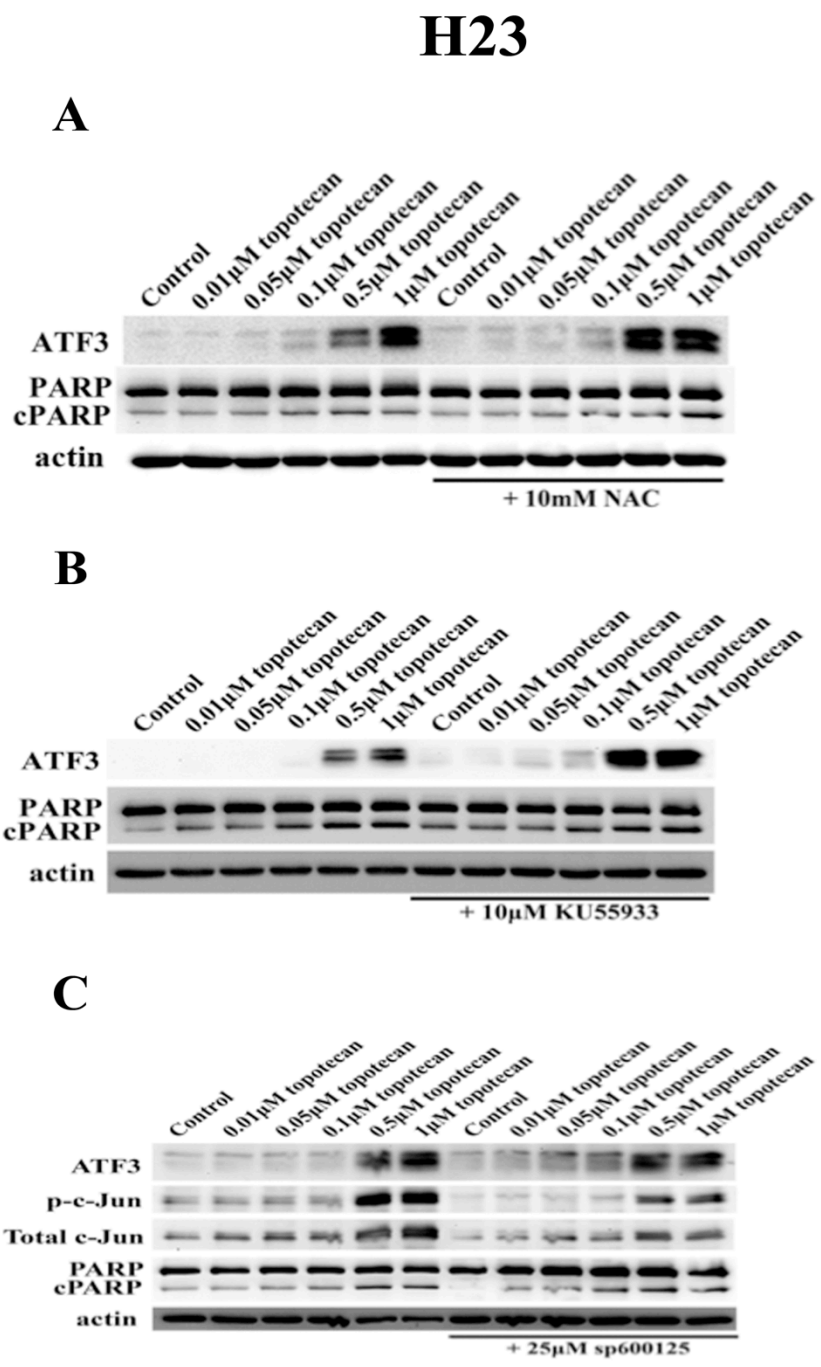

Supplemental Figure 4. Evaluating the pathways underlying topotecan cytotoxicity in the H23 cell line. H23 cells were treated with **A)** 10mM NAC, **B)** 10μM ATM inhibitor KU55933 and **C)** 25μM JNK inhibitor SP600125 prior to co-treatment with topotecan for 24 hours. Western blot analysis was performed to evaluate ATF3 expression and PARP cleavage. No pronounced attenuation in the ATF3 expression was observed following the co-treatment of topotecan with NAC, KU55933 and SP600125. Actin was used as a loading control.